On the role of planetary-scale waves in the abrupt seasonal transition of the Northern Hemisphere general circulation

Tiffany A. Shaw *

Department of Earth and Environmental Sciences &

Lamont-Doherty Earth Observatory &

Department of Applied Physics and Applied Mathematics,

Columbia University, New York, New York, USA

* *Corresponding author address:* Dr. Tiffany A. Shaw, Department of Earth and Environmental Sciences and Department of Applied Physics and Applied Mathematics, Columbia University, P.O. Box 1000, 61 Route 9W, Palisades, NY, 10964, E-mail: tas2163@columbia.edu

ABSTRACT

The role of planetary-scale waves in the abrupt seasonal transition of the Northern Hemisphere (NH) general circulation is studied. In reanalysis data the winter to summer transition involves the growth of planetary-scale wave latent heat and momentum transports in the region of monsoons and anticyclones that dominate over the zonal-mean transport beginning in mid spring. The wave-dominated regime coincides with an abrupt northward expansion of the cross-equatorial circulation. In the upper troposphere, the regime transition coincides with the growth of cross-equatorial planetary-scale wave momentum transport and a poleward shift of subplanetary-scale wave transport and jet stream.

The dynamics of the seasonal transition are captured by idealized aquaplanet model simulations with a prescribed subtropical planetary-scale wave sea surface temperature (SST) perturbation. The SST perturbation generates subtropical planetary-scale wave streamfunction variance and transport in the lower and upper troposphere consistent with QG theory. Beyond a threshold SST a transition of the zonal-mean circulation occurs, which coincides with a localized reversal of absolute vorticity in the NH tropical upper troposphere. The transition is abrupt in the lower troposphere due to the quadratic dependence of the wave transport on the SST perturbation and involves seasonal timescale feedbacks between the wave and zonal-mean flow in the upper troposphere, including cross-equatorial wave propagation. The zonal-mean vertical and meridional flow associated with the circulation response are in balance with the planetary-scale wave momentum and latent heat flux divergences. The results highlight the leading-order role of monsoon-anticyclone transport in the seasonal transition, including its impact on the meridional extent of the Hadley and Ferrel cells. They can also be used to explain why the transition is less abrupt in the Southern Hemisphere.

1. Introduction

One of the most dramatic aspects of the Northern Hemisphere (NH) seasonal cycle is the transition from quasi zonally-symmetric near-surface flow in winter to zonally asymmetric monsoons and subtropical anticyclones during summer. This transition occurs in conjunction with a dramatic expansion of the Southern Hemisphere (SH) Hadley cell, a poleward shift of the NH jet stream and upward displacement of the subtropical tropopause. The seasonal transition is associated with the onset of NH monsoons over North America, Asia, and Africa, which peak during summer and encompass longitudinal regions of upward motion over continents and downward motion over the eastern branches of subtropical anticyclones (Rodwell and Hoskins 1996; Trenberth et al. 2000; Rodwell and Hoskins 2001).

The monsoons displace the intertropical convergence zone into the subtropics and dominate the zonally averaged circulation during summer (e.g., Chao and Chen 2001; Gadgil 2003; Webster and Fasullo 2003), however their relationship to the conventional zonal-mean framework of the general circulation, including the familiar Hadley and Ferrel cells, remains unclear. Several authors have investigated the applicability of an angular momentum conserving framework, which has been applied to the Hadley circulation (e.g., Held and Hou 1980; Lindzen and Hou 1988; Plumb and Hou 1992), to describe the monsoon circulation. The framework has been shown to be useful for interpreting idealized aquaplanet model simulations in the absence of a background flow (Zheng 1998; Privé and Plumb 2007a) and predicts that the poleward boundary of the monsoon circulation should be co-located with the maximum sub-cloud moist entropy (or moist static energy) (Emanuel 1995; Privé and Plumb 2007a).

An angular momentum conserving framework excludes the possibility that eddies, defined as deviations about the zonal mean, play a role in the monsoon circulation. However, Bordoni and Schneider (2008) and Schneider and Bordoni (2008) have suggested that extratropical baroclinic eddies mediate the seasonal transition, including monsoon onset. They noted a transition between tropical circulation regimes that depend on the degree to which extratropical eddies dominated the momentum flux divergence in reanalysis data and idealized general circulation model experiments with seasonally varying solar insolation and low surface thermal inertia. During summer and in the equinox seasons the tropical circulation is eddy dominated whereas during winter the flow is closer to angular momentum conserving.

In a zonal-mean framework the monsoon-anticyclone system can be considered as a planetary-scale Rossby wave driven by land-ocean heating asymmetries (following Gill 1980) with associated planetary-scale wave transport. Several authors have noted significant quasi-stationary planetary-scale wave momentum transport in the tropical upper troposphere during NH summer (e.g., Lee 1999; Dima et al. 2005). The planetary-scale wave transport produces an eastward acceleration that is balanced by a westward acceleration due the cross-equatorial Eulerian-mean meridional circulation, which maintains westward flow in the tropical upper troposphere (see Fig. 11 in Dima et al. 2005). Dima et al. (2005) showed that the structure of the planetary-scale wave transport is consistent with the response of the nonlinear shallow water equations to a zonally-asymmetric off-equatorial heating suggesting that the tropical wave transport is connected to heating in the summer hemisphere. Kelly and Mapes (2011, 2013) showed that subtropical stationary wave momentum transport associated with the upper tropospheric Tibetan anticyclone modulates North American drought through an impact on the North Atlantic subtropical anticyclone. Finally, Shaw and Pauluis (2012) showed that latent heat transport in the vicinity of subtropical anticyclones and monsoons dominates the mass transport by the NH summer circulation in isentropic coordinates.

These previous studies have highlighted the importance of quasi-stationary planetary-scale waves in the general circulation during summer. It is well known that forced stationary waves interact with the Hadley circulation during NH winter (e.g., Held and Phillips 1990; Caballero 2008). Here I seek to understand the role of planetary-scale waves in the seasonal transition of the NH general circulation, including their impact on the evolution of the Hadley cell, Ferrel cell, and jet stream. Relevant questions include: Can a zonally-asymmetric perturbation produce a transition of the zonal-mean circulation? How is the transition different from zonally-symmetric angular momentum conserving flows? Understanding how the monsoon-anticyclone system fits into conventional theories of the general circulation, including zonally-symmetric tropical (e.g., Held and Hou 1980) and extratropical eddy-driven (see Schneider 2006) theories, is important for improving our understanding of monsoon onset and for interpreting the response of the Eulerian-mean circulation to climate change.

The paper is organized as follows. Section 2 discusses the data and model simulations used in this study. In section 3 the seasonal cycle of the general circulation and planetary-scale wave transport in reanalysis data is presented. The reanalysis data show the coherent growth of lower tropospheric planetary-scale wave transport from winter to summer that marks the transition to a planetary-scale wave dominated regime. In section 4 idealized aquaplanet model simulations are used to examine whether a planetary-scale zonally asymmetric subtropical forcing can produce a regime transition of the zonal-mean circulation. The model experiments illustrate the transition from a zonally-symmetric circulation to a circulation dominated by stationary wave latent heat and momentum transports. The circulation transition is abrupt beyond a threshold forcing amplitude and involves seasonal timescale wave-mean flow interaction in the upper troposphere. Section 5 includes a summary and discussion.

2. Tools

a. Reanalysis data

The seasonal evolution of the general circulation and wave transport in the real atmosphere is assessed using European Centre for Medium-Range Weather Forecasts (ECMWF) Interim (ERA-Interim) data set from 1979 to 2012 (Dee et al. 2011). The daily zonal u, meridional v and vertical ω wind, temperature T and specific humidity q are provided on a 1.5° by 1.5° horizontal grid on 37 pressure levels. In all cases waves are defined as deviations from the daily zonal mean e.g., $[u^*v^*] = [uv] - [u][v]$, with brackets denoting zonal averages, following Peixoto and Oort (1992). As in Shaw and Pauluis (2012) I convert moisture transport to latent heat transport by multiplying by L_v/c_p, where L_v is the latent heat of vaporization and c_p is the specific heat at constant pressure. I also label the transport according to a zonal wavenumber k decomposition: transport by the zonal-mean, including the Hadley and Ferrel cells, is defined as $k = 0$ e.g., $[u][v]$, planetary-scale wave transport is defined as $1 \leq k \leq 3$ e.g., $[u^*v^*]_{1\leq k\leq 3}$, and finally subplanetary-scale (synoptic-scale) transport is defined as $k \geq 4$ e.g., $[u^*v^*]_{k\geq 4}$. Note that the planetary-scale wave transport is highly correlated with stationary wave transport defined as a deviation about the monthly mean. In all cases the daily seasonal cycle is smoothed using a 10-day moving average.

b. General circulation model

Idealized fixed sea surface temperature (SST) aquaplanet model experiments are performed using the Community Atmosphere Model (CAM) version 5.0 general circulation model (Neale et al. 2010). An aquaplanet model configuration was chosen because it is an idealized setting that includes moisture transport, which plays an important role in the seasonal cycle (Shaw and Pauluis 2012). The simulations employ the CAM version 3.0 physics package (Collins et al. 2006) to avoid complications resulting from interactive aerosols. A zonally-symmetric SST is prescribed according to the "Qobs" profile of Neale and Hoskins (2001). A zonal wavenumber-2 perturbation is added to the zonally-symmetric basic state at 30°N to mimic subtropical land-ocean heating asymmetries, including land cyclones and ocean anticyclones during NH summer[1]. All simulations are run for 10 years but the equilibrium state is achieved within the first year.

Many previous studies used dry dynamical models to explore the impact of imposed zonally-asymmetric diabatic heating perturbations in the absence or in the presence of a basic state (e.g., Gill 1980; Rodwell and Hoskins 2001; Kraucunas and Hartmann 2005, 2007). Our approach is complementary to previous studies that used idealized aquaplanet

[1] A wavenumber-1 perturbation was also considered and the results were in qualitative agreement with those discussed below.

models to understand monsoon dynamics (Privé and Plumb 2007a,b; Bordoni and Schneider 2008). However, here I focus on the impact of surface zonal asymmetries, via wave latent heat and momentum transport, on a zonally-symmetric basic state Eulerian-mean meridional circulation.

3. Seasonal transition in reanalysis data

Here I establish the main features of the seasonal transition in reanalysis data, which motivate the aquaplanet experiments described in the subsequent section. As discussed in the Introduction, the NH exhibits a dramatic transition between winter and summer. Figure 1 shows the seasonal cycle of the zonal-mean vertical and zonal wind at 900 hPa (top) and zonal-mean meridional and zonal wind at 150 hPa (bottom). The main features of the NH transition are: the northward expansion of zonal-mean upwelling into the NH subtropics and development of equatorial downwelling (top, left), the weakening of the meridional flow in the NH Hadley cell (bottom, left), the transition toward eastward flow in the NH tropical lower troposphere (top, right) and westward flow in the tropical upper troposphere (bottom, right) and the northward shift of the NH jet stream. Note that the northward shift of zonal-mean upwelling and transition to zonal-mean eastward near surface flow in the tropics are zonal-mean signatures of monsoon onset.

The seasonal transition of the zonal-mean flow is coupled to significant changes in the planetary-scale wave transports that reflect the growth of zonal asymmetries (Fig. 2, left). The seasonal cycle of $L_v[v^*q^*]_{1\leq k\leq 3}/c_p$ (Fig. 2 top, left) and $[u^*v^*]_{1\leq k\leq 3}$ (Fig. 2 middle, left) in the lower troposphere (900 hPa) are synchronized and exhibit a dramatic increase with maxima around day 167 (June 16), consistent with Shaw and Pauluis (2012). The magnitude of the transports are sufficient to dominate over the zonal-mean transport beginning in mid-spring (see shading)[2]. The dominance of northward latent heat transport in the NH

[2]The shaded regions indicate where the Péclet number defined as $Pe = |[v][q]|/|[v^*q^*]_{1\leq k\leq 3}|$ and Reynolds number defined as $Re = |[u][v]|\ /\ |[u^*v^*]_{1\leq k\leq 3}|$ are < 1 (in regions where the denominator is non zero).

subtropics during summer is striking because the transport in low latitudes is typically toward the ascending branch of the Hadley circulation, which would be southward in the NH subtropics during summer.

The planetary-scale wave latent heat flux divergence (Fig. 2, top, right) is associated with transport between the tropics and subtropics and dominates over the flux divergence by the zonal-mean flow (see shading). Its evolution is directly coupled to the zonal-mean upwelling: the region of zonal-mean upwelling shifts northward by 10 degrees just prior to the wave transport maximum and its northward boundary subsequently coincides with the maximum transport (i.e., zero planetary-scale wave latent heat flux divergence). Around the same time there is a transition toward zonal-mean equatorial downwelling. The connection between zonal-mean vertical motion and planetary-scale wave latent heat flux divergence is suggestive of wave-mean flow interaction via the following balance, $[\omega]\, \partial_p[q] \approx -\partial_\phi(\cos\phi\, [v^* q^*])/a\cos\phi$. This balance seems to account for the northward shift of zonal-mean upwelling and the development of the local upwelling maximum at 20°N that marks the poleward boundary of the cross-equatorial circulation.

According to quasiequilibrium theory, the poleward boundary of the cross-equatorial zonal-mean circulation (i.e., SH Hadley cell) should be co-located with the maximum zonal-mean sub-cloud moist entropy (or moist static energy) i.e., $\partial[\theta_e]/\partial\phi \approx 0$ (Emanuel 1995; Privé and Plumb 2007a). The maximum zonal-mean moist entropy at 900 hPa (green line in Fig. 2, top, right) is located around 10°N during NH summer and thus does not coincide with the northward boundary of the circulation, which occurs around 20°N. The boundary of the cross-equatorial circulation is associated with a local upwelling maximum at 20°N that closely follows the maximum planetary-scale wave latent heat transport (as discussed above) and the maximum planetary-scale wave moist entropy variance[3] (Fig. 2, bottom).

[3]The dominant terms in the wave moist entropy variance in the NH subtropics are the wave latent heat variance $L_v^2 \left[{q^*}^2\right]/c_p^2$, which is positive, and the correlation between the wave latent and sensible heat $L_v[q^*\theta^*]/c_p$, which is negative reflecting regions of dry, warm air over deserts.

The evolution suggests that the poleward boundary of the cross-equatorial circulation is co-located with the maximum planetary-scale waviness in the lower troposphere.

In addition to transporting latent heat between the tropics and subtropics, planetary-scale waves also transport momentum between the tropics and subtropics (Fig. 2, middle). The planetary-scale wave momentum flux divergence does not play a dominant role in the evolution of the near-surface zonal-mean flow. The near surface zonal-mean flow is determined by a balance between the Coriolis force and surface friction, which also changes sign during the transition (not shown).

While the tropical and subtropical planetary-scale wave transport in the lower troposphere peaks during NH summer and is weak otherwise, the upper-tropospheric (150 hPa) planetary-scale wave momentum transport is large in the NH during much of the seasonal cycle (Fig. 3, top, left). During winter there is well-known extratropical stationary wave momentum transport (Randel and Held 1991; Held et al. 2002) that impacts the Hadley circulation (Held and Phillips 1990; Caballero 2008). Consistent with the lower tropospheric transport, $[u^*v^*]_{1\leq k\leq 3}$ dominates over the zonal-mean transport during much of the seasonal cycle in the NH (see shading). At upper levels the key feature of the transition from winter to summer is the growth of northward cross-equatorial planetary-scale wave momentum transport that reaches a maximum at 5°S around day 210 (July 29), which is approximate 50 days later than the maximum in the lower troposphere. Note that cross-equatorial momentum transport suggests southward wave propagation. The planetary-scale wave transport evolution is coupled to a 10 degree poleward shift of the subplanetary-scale transport $[u^*v^*]_{k\geq 4}$ (Fig. 3, left, middle)[4]. The zonal-mean transport by the winter (SH) Hadley cell only dominates between 15 and 25°S (region without gray shading in Fig. 3 top, left).

The seasonal evolution of upper tropospheric planetary-scale wave momentum transport in the NH tropics and subtropics is consistent with the evolution of the zonal-mean meridional

[4]The shading indicates regions where $([u][v] + [u^*v^*]_{1\leq k\leq 3})/[u^*v^*]_{k\geq 4} < 1$ and thus where subplanetary-scale transport dominates over the other components.

flow (Fig. 3 top, right). This consistency reflects a balance in the zonal momentum budget of $-f[v] \approx -\partial_\phi(\cos^2\phi\ [u^*v^*]_{1\le k\le 3})/a\cos^2\phi$, where f is the Coriolis parameter and the other symbols have their usual meaning (see Dima et al. 2005). In mid and high latitudes the momentum balance is $-f[v] \approx -\partial_\phi(\cos^2\phi\ [u^*v^*]_{k\ge 4})/a\cos^2\phi$. The subplanetary-scale wave momentum flux divergence exhibits a poleward shift (Fig. 3, middle, right) consistent with the shift of the NH jet stream (see Fig. 1 right). Finally, in the SH tropics the momentum balance is $-f[v]+[v]\ \partial_\phi(\cos\phi\ [u])/a\cos\phi \approx -\partial_\phi(\cos^2\phi\ [u^*v^*]_{1\le k\le 3})/a\cos^2\phi$ (Fig. 3, bottom, right) suggesting the flow does not conserve angular momentum.

Overall, the ERA-Interim reanalysis data suggest a seasonal transition in the NH toward a planetary-scale wave dominated regime. The key features of NH climate during June, July, and August (JJA) are shown in Fig. 4. During JJA there is a weak NH Hadley cell, a broad SH Hadley cell, and a strong NH moist isentropic circulation, which Shaw and Pauluis (2012) showed was due to stationary wave latent heat transport. In addition, there is westward flow in the tropical upper troposphere and a poleward shifted NH jet stream. These mean flow characteristics coincide with significant zonal-mean planetary-scale wave latent heat and momentum transports in the lower troposphere and two distinct upper tropospheric momentum transport maxima (Fig. 4, bottom). The planetary-scale wave transport coincides with planetary-scale wave streamfunction variance (not shown). The lower-tropospheric latent heat transport occurs in the region of monsoon cyclones and subtropical anticyclones (Fig. 5, left). The equatorward flow of relatively dry air on the eastern side of the Atlantic and Pacific ocean basins as well as in the eastern Saharan and Arabian deserts leads to poleward latent heat transport. The poleward flow of relatively dry air in the vicinity of the Somali jet produces southward cross equatorial transport (Held and Czaja 2012). The momentum transport in the upper troposphere exhibits a quadrupole pattern consistent with the Tibetan anticyclone that is coupled to cross-equatorial momentum transport, which peaks in the SH tropics (Fig. 5, right). The role of monsoon-anticyclone transport in the abrupt seasonal transition of the NH general circulation is explored using idealized aquaplanet model experiments in the next section.

4. Aquaplanet model simulations

Here the CAM5 aquaplanet model (see Section 2b) is used to understand how the general circulation responds to a subtropical zonally-asymmetric surface forcing. The CAM5 basic state SST is the zonally-symmetric 'Qobs' SST of Neale and Hoskins (2001) with the maximum SST shifted to 10°N, which mimics the northward shift of solar insolation during late spring (Fig. 6 top, left). [The northward shift also prevents superrotation (see Kraucunas and Hartmann 2005).] The zonally-symmetric circulation associated with the SST exhibits a strong SH Hadley Cell and a weak NH Hadley cell (Fig. 6 bottom, left), consistent with the symmetry breaking that occurs when zonal-mean heating is shifted off of the equator (Lindzen and Hou 1988; Plumb and Hou 1992). The SH Hadley cell and subtropical jet stream are stronger than in reanalysis data, which is common for aquaplanet models, especially those that are not coupled to a slab ocean (Frierson et al. 2006). The moist isentropic circulation in the NH is stronger than the corresponding Eulerian-mean circulation (compare Fig. 6 bottom, left and right).

I hypothesize that a stationary Rossby wave driven by subtropical land-ocean heating asymmetries (sensible and latent heating over land and long-wave radiative cooling over the ocean) can produce an abrupt transition of the general circulation. To test this I introduce a surface zonal asymmetry in the aquaplanet model via a wave-2 SST perturbation centered at 30°N (Fig. 6 top, right) and vary its amplitude from 0 to 10 K. The increasing SST mimics the build up of subtropical waviness and associated wave transport during the seasonal cycle. I am interested in whether this simple configuration can capture the features of the NH seasonal transition, namely increasing planetary-scale wave transport in the lower and upper troposphere, weakening of the NH Hadley cell, expansion of the SH Hadley circulation into the NH, and poleward shift of the NH jet stream.

When the wave-2 SST amplitude is increased a surface cyclone/anticyclone pattern develops over the warm/cold SST regions. The amplitude of the cyclone/anticyclone pattern, as measured by the zonal-mean wave-2 streamfunction variance $[\psi^*\psi^*]_{k=2}$, increases quadratically for wave-2 SST amplitudes ≤ 8 K and subsequently saturates (not shown). The wave-2 latent heat and momentum transports in the subtropical lower troposphere increase linearly with increasing wave-2 streamfunction variance for SST amplitudes ≤ 8 K (Fig. 7 top, left). These relationships imply the wave-2 transport increases quadratically as a function of wave-2 SST, thus a small increase in SST forcing produces a large increase in wave transport. The linear relationship between wave transport and streamfunction variance is consistent with quasi-geostrophic (QG) theory. According to QG theory, $[u^*v^*] = -k\ell\ [\psi^*\psi^*]$ where k and ℓ are the zonal and meridional wavenumbers, respectively. Recall that ℓ depends on $\beta^* = \beta - [u]_{yy}$. The linear relationship in Fig. 7 (top, left) implies that ℓ is constant (recall that k is fixed) and the positive slope indicates southward propagation (i.e., $\ell < 0$). The relationship between wave-2 latent heat transport and streamfunction variance is expected to depend on k and the vertical wavenumber m consistent with its treatment as a thermodynamic variable similar to temperature (sensible heat). Recall that according to QG theory $[v^*T^*] = \rho km[\psi^*\psi^*]/N^2$ where ρ is density, N is the buoyancy frequency, and m depends on the vertical zonal wind shear. The linear relationship between latent heat transport and streamfunction variance suggests upward propagation.

The wave-2 SST perturbation in the subtropical lower troposphere remotely impacts the upper tropospheric wave-2 streamfunction and transport in the NH subtropics (20 to 40°N) and tropics (20°S to 20°N) (Fig. 7 top, right). For small wave-2 SST amplitudes the subtropical wave-2 momentum transport is linearly related to the wave-2 streamfunction variance but for SST amplitudes ≥ 6 K the transport saturates. In the subtropical upper troposphere a deviation from linearity is expected because of wave-mean flow interaction. In particular, the zonal-mean zonal flow can affect wave propagation and transport via changes in the zonal wind and thus the meridional wavenumber. Conversely, the wave momentum flux convergence can affect the zonal-mean flow. The saturation of the subtropical wave-2 momentum transport coincides with a poleward shift of the NH jet (see Fig. 7, middle, right) that acts to decrease the meridional wavenumber locally and accounts for the saturation of the wave-2 momentum transport. In contrast to the subtropical transport, the linear relationship between wave-2 streamfunction variance and transport holds in the tropical upper troposphere suggesting that wave-2 momentum transport in that region is directly controlled by wave-2 streamfunction variance. The dynamical mechanism that accounts for tropical wave variance in response to a subtropical forcing is discussed below.

The Eulerian-mean circulation mass transport defined as $\Delta\Psi(\phi) = \max_p \Psi - \min_p \Psi$ exhibits a clear transition as a function of wave-2 SST amplitude (Fig. 7 middle, left). For wave-2 SST amplitudes < 6 K the dominant response is a weakening of the NH Hadley cell. For wave-2 SST amplitudes ≥ 6 K there is a northward shift of the edge of the SH Hadley cell (see red line Fig. 7 bottom, left), a contraction of the NH Hadley cell and a northward shift of the NH Ferrel cell. The northward shift of the edge of the SH Hadley cell is quite dramatic between 6.5 and 8 K, consistent with the quadratic dependence of the wave-2 streamfunction variance on the wave-2 SST. The Eulerian-mean circulation mass transport response scales linearly with the standard deviation of the wave-2 streamfunction (not shown).

The response of the Eulerian-mean circulation suggests that a circulation transition occurs for a 6 K wave-2 SST amplitude, which I label the "threshold SST". The Eulerian-mean circulation response beyond the threshold SST is consistent with poleward shifts of the subtropical (defined at 200 hPa) and eddy-driven (defined at 850 hPa) jet maxima in the NH (Fig. 7 middle, right). The connection between the jet shifts and wave-2 transport is discussed below. The threshold SST amplitude depends on the treatment of convection: the SH Hadley cell broadening occurs for higher SST values in simulations without a convective parameterization (i.e., only large-scale condensation, not shown).

The northward shift of the SH Hadley cell edge beyond the threshold SST does not coincide with a northward shift of the maximum zonal-mean sub-cloud moist entropy, as would be expected from quasiequilibrium theory. Instead the maximum zonal-mean sub-cloud moist entropy moves southward with increasing wave-2 SST amplitude (Fig. 7 bottom, left, solid line). The southward shift results from a flattening of the subtropical zonal-mean sub-cloud moist entropy meridional gradient due to wave-2 latent heat transport between the tropics and subtropics. While the maximum zonal-mean sub-cloud moist entropy moves southward with increasing wave-2 SST amplitude, the global moist entropy maximum moves northward (Fig. 7 bottom, left, dashed line). Note however that the northward movement of the global maximum does not coincide with the threshold SST (it occurs for wave-2 SST $\geq$ 2.5 K). In the zonal-mean framework zonally localized increases in moist entropy are reflected in the wave moist entropy variance (not shown).

The threshold SST, which marks the transition of the zonal-mean circulation, coincides with a localized reversal of absolute (vertical) vorticity ζ_a in the NH tropical upper troposphere at 150 hPa (Fig. 7 bottom, right, dashed line). The negative absolute vorticity occurs in the NH tropics at 25°W and 155°E and coincide with an angular momentum maxima. Negative zonal-mean absolute vorticity, i.e., $[\zeta_a] < 0$, in the upper troposphere is the threshold criteria for the transition to a thermally direct zonally-symmetric circulation (Plumb and Hou 1992). Schneider (1987) and Emanuel (1995) showed how the result could be extended to non-symmetric and moist flows that satisfy QG dynamics. In the aquaplanet model simulations the zonal-mean absolute vorticity does not reverse (Fig. 7 bottom, right, solid line). Additional experiments with corresponding zonal-mean SST forcings did not produce a reversal of zonal-mean absolute vorticity. However in response to a zonal-mean forcing the edge of the cross-equatorial circulation does coincide with the zonal-mean sub-cloud moist entropy (not shown). The connection between the reversal of absolute vorticity and the stationary wave response in the upper troposphere is discussed below.

The aquaplanet experiments show that in response to increasing subtropical wave-2 SST amplitude, and thus wave-2 streamfunction variance and transport, the zonal-mean circulation undergoes a transition involving the broadening of the SH Hadley cell, the weakening of the NH Hadley cell and a poleward shift of the NH jet – three key features of the seasonal transition in reanalysis data. The Eulerian-mean meridional circulation and zonal-mean zonal wind response below (5.5 K) and above (7.5 K) the wave-2 SST threshold along with the difference from the background state are shown in Fig. 8. Below the threshold the circulation response is weak but non zero, however above the threshold there is a strong vertically deep counter-clockwise circulation near the equator. In addition there is a clockwise circulation in the upper troposphere that is connected to a poleward shift of the Ferrel cell in the extratropics. The zonal-mean zonal wind response above the SST threshold displays a number of similarities with reanalysis data, in particular the zonal wind in the tropical upper troposphere is westward and the surface zonal wind in the NH tropics is weakly eastward, indicating a reversal of the trade winds. There is a also a clear poleward jet shift in the NH and a raising of the subtropical tropopause.

Beyond the threshold SST the moist isentropic circulation is significantly stronger than and the opposite sign of the corresponding Eulerian-mean circulation (compare Figs. 8 and 9). In order to understand the differences between the circulation responses I appeal to the statistical transformed Eulerian-mean (STEM) formulation (Pauluis et al. 2011). The STEM formulation is based on a Gaussian distribution assumption for the meridional mass transport and can be used to decompose the moist isentropic circulation into Eulerian-mean and eddy-driven components. Wu and Pauluis (2013a) showed the STEM can be used to understand the circulation response to external forcing such as a doubling of carbon dioxide [see their equations (6)-(9)]. When applied to the current aquaplanet model experiments, the STEM decomposition suggests that the Eulerian-mean circulation response dominates in the NH tropics. In contrast, the response in the SH tropics is due to the upward shift of the vertical coordinate i.e., the rise of the tropopause. Finally, in the NH subtropics where the moist isentropic and Eulerian-mean circulation responses differ in sign, the STEM formulation shows that the strong clockwise moist isentropic circulation is due to a combination of poleward wave-2 latent heat transport and wave-2 latent heat variance. Recall that eddy latent heat transport is included in the meridional mass transport in moist isentropic coordinates. The results agree with Shaw and Pauluis (2012) who showed that the NH summer circulation is dominated by stationary planetary-scale latent heat transport (see their Fig. 15). The STEM analysis suggests that planetary-scale wave transport and variance play a key role in the subtropical circulation response to zonally-asymmetric forcing.

a. Eddy transport response

In order to understand the dynamics of the zonal-mean circulation response to the wave-2 SST forcing I begin with an examination of the wave-2 transport response. The subtropical wave-2 SST perturbation generates a stationary Rossby wave that exhibits a baroclinic vertical structure and satisfies Sverdrup vorticity balance (not shown), consistent with reanalysis data (Chen 2003, 2010). Beyond the threshold SST the stationary wave activity as measured by wave-2 streamfunction variance occurs in three distinct locations: NH tropical lower troposphere, NH subtropical and tropical upper troposphere (Fig. 10, top, left). The wave-2 streamfunction variance in the NH subtropical lower troposphere is the QG response to the wave-2 SST and scales quadratically with the SST amplitude, as discussed previously. The NH subtropical upper troposphere is directly coupled to the lower troposphere via the baroclinic vertical structure of the Rossby wave (the cyclone/anticyclone pattern is 180 degrees out of phase with the surface pattern). The wave-2 streamfunction variance in the tropical upper troposphere is non-local to the subtropical wave-2 forcing. The dynamics of the tropical response are discussed below.

The wave-2 streamfunction variance leads directly to latent heat and momentum transports and latent heat variance (Fig. 10) following QG theory. The wave-2 transports in the lower troposphere scale linearly with the subtropical wave streamfunction variance, as discussed previously (see Fig. 7). The wave-2 transports are sufficient to dominate over the zonal-mean transport in the NH tropics and subtropics (see shading) consistent with reanalysis data (see Figs. 2 and 3). Overall the wave transport beyond the SST threshold is very consistent with reanalysis data.

The zonal structure of the lower tropospheric (900 hPa) stationary-wave latent heat transport response to 5.5 K and 7.5 K wave-2 SST forcings is shown in Fig. 11 (top). The stationary wave latent heat transport is consistent with the cyclone/anticyclone meridional flow as indicated by the streamfunction (black). The transport is largest for the cyclones, which have the strongest amplitude and dominate the zonal-mean transport. Note that the aquaplanet simulations do not capture the poleward latent heat transport in the region of equatorward flow seen in reanalysis data (see Fig. 4 and Shaw and Pauluis 2012). Note that this leads to weaker zonal-mean transport.

The zonal structure of the upper tropospheric (150 hPa) stationary wave momentum transport (color) response to 5.5 K and 7.5 K wave-2 SST forcing is shown in Fig. 11 (bottom). The wave momentum transport for the 5.5 K SST exhibits a quadrupole pattern consistent with the dominant upper level anticyclone. The maximum transport occurs in the south-east section of the anticyclone in the region of equatorward flow. The tropical wave-2 momentum transport (and wave-2 streamfunction variance) moves southward with increasing wave-2 SST. For 7.5 K it peaks on the equator and extends into the SH tropics consistent with reanalysis data (Fig. 4, right). The southward shift of the momentum transport for 7.5 K SST coincides with increased equatorward and westward flow (magenta line indicates zero zonal wind) suggesting that the stationary wave propagates across the equator through a region of westward flow. Recall that the zero zonal wind line represents a critical layer for stationary waves, according to linear theory (Charney and Drazin 1961), and thus a meridional bound on the momentum transport. Thus, the wave-2 momentum transport appears to violate linear theory.

While the relationship between the upper tropospheric momentum transport and zero zonal-wind line appears to violate linear theory, the prediction that the critical layer should bound wave transport is derived in the absence of an Eulerian-mean circulation. Schneider and Watterson (1984) showed that in the presence of a zonal-mean meridional flow stationary wave propagation is permitted in the direction of the flow even in the presence of the critical layer. Kraucunas and Hartmann (2007) noted cross-equatorial propagation in a nonlinear shallow water model with an imposed zonal-mean meridional flow. The dispersion relation for the barotropic vorticity equation with imposed zonal-mean zonal and meridional wind is

$$[v]\ell(k^2+\ell^2)/k + ([u]-c)(k^2+\ell^2) - \beta^* = 0 \quad (1)$$

and the meridional group velocity is

$$c_{gy} \quad = \quad [v] + \frac{2\beta^* k\ell}{(k^2+\ell^2)^2} \quad (2)$$

(see eqns. (15) and (22) in Schneider and Watterson 1984). Note (1) reduces to the usual stationary Rossby wave dispersion relation when $c = [v] = 0$. Schneider and Watterson (1984) showed that if $[v] \neq 0$ and $[v]^2 < [u]^2/3$ then there exists three distinct propagating solutions (see their Section 4). At a critical layer where $[u] = 0$ only one propagating solution exists and if $[v] < 0$ then the lines of constant phase for that solution should tilt south-west to north-east.

Overall, the upper level wave streamfunction in the aquaplanet simulations is very consistent with linear wave propagation in the presence of a southward flow e.g., the linear propagation criteria are satisfied and the phase tilt is consistent. Note that southward wave propagation accounts for the stationary wave streamfunction variance in the tropical upper troposphere. In addition the southward mean flow is maintained by wave-2 momentum flux divergence, as discussed below, suggesting significant wave-mean flow interaction.

The dynamics of the upper tropospheric stationary wave propagation are directly coupled to the changes in the Eulerian-mean circulation. Recall that the northward shift of the edge of the cross-equatorial circulation (SH Hadley cell) to the wave-2 SST forcing coincides with a reversal of the absolute vorticity in the NH (see Fig. 7, bottom, left). Beyond the SST threshold the geostrophically balanced flow associated with the upper tropospheric wave-2 streamfunction is sufficient to reverse the absolute vorticity in the NH tropics south of the upper-level cyclones (i.e., 25°W and 155°E). More specifically, $f\zeta_a \approx f^2 + \nabla^2\Phi + \beta u < 0$ where Φ is the geopotential, which reflects a balance in the divergence equation of $f\zeta_r \approx \nabla^2\Phi + \beta u$.

The ζ_a reversal occurs in the south-east section of the upper tropospheric cyclones where the flow is north-east (see green line in bottom panel of Fig. 11) and coincide with localized angular momentum maxima[5]. The north-east flow is not consistent with the zonal-mean response, which is south-west (see Fig. 8) and consistently there is no reversal of $[\zeta_a]$ (see Fig. 7 bottom, right, solid line). In general, an absolute vorticity reversal indicates the transition to a thermally direct circulation (Plumb and Hou 1992; Emanuel 1995). In the aquaplanet model simulations the reversal does not coincide with maximum divergence, which occurs in the vicinity of the upper-level anticyclone. Instead the reversal of absolute vorticity coincides with a region of weaker upper-level divergence in the NH tropics around 25°W and 155°E. It seems to be an indicator of the dominance of the planetary-scale wave circulation, including its cross-equatorial advection and angular momentum maximum. The upper level reversal of absolute vorticity is coupled to a sub-cloud moist entropy field that satisfies the non-zonally symmetric surface criteria derived by Emanuel (1995) (see his equation 25).

b. Eddy flux divergence response

The eddy transport response to the subtropical zonally-asymmetric SST forcing discussed in the previous section can be connected directly to the Eulerian-mean circulation response via the meridional flux divergence of the wave-2 transport response. Recall that beyond the threshold SST, the circulation response involves a vertically deep circulation cell in the NH tropics (see Fig. 8). Figure 12 shows the wave-2 latent heat and momentum flux divergence (top) response to the 7.5 K SST forcing. The latent heat flux divergence dipole in the lower troposphere transports heat poleward (Fig. 12 top, left) and shifts the maximum tropical zonal-mean moist entropy southward (see solid line in Fig. 7, bottom, left). The wave-2 flux divergence is consistent with the zonal-mean vertical motion response via a balance with zonal-mean vertical advection. Consistently, the boundary of the cross-equatorial circulation is slightly equatorward of the maximum wave-2 streamfunction variance (compare Fig. 8

[5]While the ζ_a reversal coincides with eastward flow at the equator the reversal does not coincide with the transition to superrotation.

bottom, left to Fig. 10, top, left).

In the NH upper troposphere the zonal-mean meridional flow associated with the circulation response is consistent with a momentum balance between the wave-2 momentum flux divergence and the Coriolis force e.g., $-f[v] \approx -\partial_\phi(\cos^2\phi\ [u^*v^*]_{k=2})/a\cos^2\phi$ (see shading in Fig. 12, top, right) as in reanalysis data. In particular, the southward flow from 0 to 20°N that produces the expansion of the SH Hadley circulation is consistent with the wave-2 momentum flux convergence. Note that this leads to a weakening of the NH Hadley cell. Recall that the wave-2 momentum transport is partly the result of cross-equatorial wave-2 propagation. The northward flow in the NH Hadley cell is balanced by the wave-2 flux momentum flux divergence between 20 to 30°N.

The wave-2 momentum flux divergence, which is locally balanced by the Coriolis force in the NH upper troposphere, must extend to the surface to satisfy the vertically integrated momentum budget (not shown). This accounts for the vertically deep counter-clockwise circulation response near the equator (see Fig. 8). The zonal-mean vertical motion associated with the circulation response is consistent with the wave-2 latent heat flux divergence via a balance with vertical advection. Thus, the northward expansion of the SH Hadley cell is due to the strengthening and interaction of the tropical circulation response due to upper level momentum transport and low-level latent heat transport.

In the SH tropics, the wave-2 momentum flux divergence interacts directly with the SH Hadley cell via the balance $|f|[v] + [v]\ \partial_\phi(\cos\phi\ [u])/a\cos\phi \approx -\partial_\phi(\cos^2\phi\ [u^*v^*]_{k=2})/a\cos^2\phi$. In response to the wave-2 momentum flux divergence, which peaks just below the tropopause, the advection by the SH Hadley cell strengthens aloft (to achieve a local balance) and the circulation shifts upward. This leads to a vertical dipole response in the momentum advection by the SH Hadley cell that accounts for the vertically shallow upper level Eulerian-mean meridional circulation response in the SH tropics (see Fig. 8, bottom, right).

The NH extratropical circulation response, which involves a poleward shift of the Ferrel cell and jet stream, is largely driven by the changes in the tropical and subtropical circulations and their impact on subplanetary-scale (synoptic-scale) wave transport. In particular, the weakening of the zonal-mean zonal flow in the NH subtropics associated with the subtropical wave-2 momentum transport leads a poleward shift of the critical layer for synoptic-scale waves. Consequently there is a poleward shift of the subplanetary-scale wave transport and eddy-driven jet stream. Recall that the jet shift occurs beyond the SST threshold consistent with the tropical circulation transition (see Fig. 7).

c. *Transient evolution*

The aquaplanet simulations demonstrate that a subtropical planetary-scale zonally-asymmetric SST perturbation can produce a transition of the zonal-mean circulation that exhibits features of the seasonal transition in reanalysis data, including the weakening of the NH Hadley cell, northward shift of the SH Hadley cell edge, poleward shift of the NH jet stream and rising of the subtropical tropopause. Recall in reanalysis data there was an abrupt transition of the zonal-mean flow in the lower troposphere and a seasonal timescale transition in the upper troposphere (see Figs. 2 and 3). Here we assess whether the aquaplanet model experiments capture the different transition timescales.

The transient response to the 7.5 K wave-2 SST forcing is shown in Fig. 13. The wave-2 latent heat transport and variance in the lower troposphere (top, left) increase rapidly and their growth coincides with a poleward shift of the zonal-mean upward motion (red line) around day 25. Note that downwelling also appears in the NH tropics. The zonal-mean vertical motion closely follows the evolution of the wave-2 latent heat variance (top, right).

In the upper troposphere the NH subtropical and tropical wave-2 momentum transport maximum increases rapidly within the first 25 days (Fig. 13 bottom, left). The maximum tropical wave-2 momentum transport migrates from the NH tropics into the SH where it reaches an equilibrium latitude of $\approx 2°$S around day 100 (Fig. 13, bottom left). The maximum subplanetary-scale wave momentum transport begins to shift poleward in the first 50 days and migrates approximately 10 degrees over the next 50 days (bottom, right).

This poleward migration closely follows the zero line of the zonal-mean zonal wind (blue line) and coincides with a poleward shift of the NH jet stream.

The seasonal timescale (≈ 50 day) adjustment in the upper troposphere is consistent with wave-mean flow interaction. The wave-2 momentum transport in the upper troposphere is consistent with zonal-mean southward flow in the SH Hadley cell, which promotes southward wave propagation via zonal-mean meridional advection. This generates wave momentum flux divergence, which strengthens the southward zonal-mean meridional flow creating a positive feedback. Similarly, the wave-2 momentum forcing weakens the NH Hadley cell and drives westward flow, which shifts the critical layer for the subplanetary-scale waves poleward producing a poleward jet shift. The aquaplanet model simulations clearly capture the transition timescales seen in reanalysis data.

5. Summary and Discussion

a. Summary

The role of planetary-scale waves in the abrupt seasonal transition of the NH general circulation is investigated. In ERA-Interim reanalysis data the seasonal transition from winter to summer is associated with the well-known weakening of the NH Hadley cell, northward expansion of the SH Hadley cell, transition to zonal-mean eastward and westward flow in the lower and upper troposphere, respectively, and a poleward shift of the NH jet stream. The present analysis has revealed the following additional features.

- The winter to summer transition involves the growth of planetary-scale wave streamfunction variance, including wave latent heat and momentum transports, in the region of monsoons and subtropical anticyclones. The wave transport dominates the zonal-mean transport beginning in mid spring. The dominance of northward latent heat transport in the NH subtropics during summer is striking because in low latitudes the transport is typically toward the ascending branch of the Hadley circulation.
- The growth of low-level transport is synchronized with an abrupt northward shift

of zonal-mean upwelling and the development of downwelling at the equator. The poleward boundary of upward motion coincides with the maximum planetary-scale wave latent heat transport or moist entropy variance.

- The transition in the lower troposphere is synchronized with cross-equatorial planetary-scale wave momentum transport in the upper troposphere that has been noted in previous studies (e.g., Lee 1999; Dima et al. 2005). At upper levels the transition occurs on a seasonal timescale (the maximum momentum transport in the upper troposphere lags the lower tropospheric maximum by approximately 50 days).
- The growth of upper-level planetary-scale wave transport coincides with a 10 degree poleward shift of subplanetary-scale wave momentum transport that occurs in conjunction with a poleward shift of the NH jet stream and Ferrel cell.

Idealized aquaplanet model simulations with a prescribed subtropical zonally-asymmetric planetary-scale SST perturbation capture the dynamics of the seasonal transition in reanalysis data. The simulations were conducted with NCAR's CAM5 model. For a sufficiently large subtropical zonally-asymmetric planetary-scale SST perturbation, the aquaplanet climate transitions from a zonally-symmetric background state to a stationary-wave dominated circulation that exhibits features of the NH summer circulation in reanalysis data.

The transition in the aquaplanet model is consistent with the interaction of a forced subtropical stationary Rossby wave with the zonal-mean flow. The interaction is summarized as a schematic in Fig. 14. The important features are

- A zonally-asymmetric subtropical forcing produces stationary wave streamfunction variance in the lower and upper troposphere. In the lower troposphere the streamfunction variance is the direct adjustment to the forcing, while in the subtropical upper troposphere it results from the wave's vertical baroclinic structure. In the upper troposphere cross-equatorial wave streamfunction variance results from southward wave propagation through a layer with westward and southward flow that is consistent with linear theory (Schneider and Watterson 1984).

- The wave streamfunction variance generates wave moisture and momentum transport consistent with QG theory. In the lower troposphere, the latent heat transport moves the maximum sub-cloud zonal-mean moist entropy maximum southward. In contrast the edge of the cross-equatorial circulation moves northward and coincides with the maximum stationary wave streamfunction variance. Upper tropospheric wave momentum transport occurs in the NH subtropics and in the SH via cross-equatorial wave propagation.

- Beyond the threshold SST of 6 K the upper tropospheric wave streamfunction is sufficient to reverse the absolute vorticity in the NH tropics and produces a localized angular momentum maximum. The reversal coincides with an abrupt northward shift of the boundary of the cross-equatorial circulation and reflects the transition of the Eulerian-mean circulation to a planetary-scale wave dominated regime.

- The flux divergence of planetary-scale wave momentum and latent heat transports are consistent with the Eulerian-mean circulation response, including upwelling in the NH subtropics, southward flow in the upper troposphere and downwelling near the equator. The dominance of planetary-scale wave latent heat transport is reflected in the strength of the moist isentropic circulation and is consistent with reanalysis data (see Shaw and Pauluis 2012). The wave transport (or streamfunction variance maximum) determines the boundary of the Hadley and Ferrel cells and shifts the tropopause upward. The raised tropopause is consistent with the connection between surface equivalent potential temperature variance and tropopause height that has been noted in previous studies (e.g., Juckes 2000; Frierson et al. 2006; Wu and Pauluis 2013b).

- The tropical circulation response associated with the stationary wave forcing decelerates the zonal wind in the NH subtropics producing a poleward shift of the critical layer for synoptic-scale waves and consequently the NH jet stream and Ferrel cell.

b. *Discussion*

Overall the present results show that the zonally-asymmetric monsoon-anticyclone system plays an important role in the seasonal transition of the NH general circulation. The impact of zonal asymmetries was identified in the zonal-mean framework as planetary-scale wave transport. The aquaplanet model simulations demonstrate that a subtropical zonally-asymmetric forcing and its associated planetary-scale wave transport can produce a transition of the zonal-mean circulation associated with abrupt changes in upward motion. Tropical circulation regime transitions have been noted in models with zonally-symmetric boundary conditions. Bordoni and Schneider (2008) noted a tropical circulation transition between angular momentum conserving and extratropical baroclinic wave dominated regimes in idealized general circulation model experiments with seasonally varying solar insolation and low surface thermal inertia.

While both zonally-symmetric and zonally-asymmetric surface forcings produce circulation transitions, here I note features that are unique to zonally-asymmetric forcings. In particular, the circulation transition in response to a zonally-asymmetric forcing coincides with the reversal of upper level absolute vorticity and an angular momentum maximum. The reversal occurs in the vicinity of the north-east flow of the upper level cyclone; not in the vicinity of the anticyclone as has been discussed previously (Plumb 2007). Furthermore, in response to an asymmetric forcing there is poleward latent heat transport, which is depends quadratically on the forcing amplitude and is directed away from the intertropical convergence zone (ITCZ). The edge of the cross-equatorial circulation coincides with maximum planetary-scale streamfunction variance and not with maximum zonal-mean sub-cloud moist entropy. Finally, the thermally direct circulation response to a zonally-asymmetric forcing does not conserve angular momentum. The reanalysis data support the role of planetary-scale waves in the seasonal transition, including the dominance of latent heat and momentum transports and the reversal of absolute vorticity (and potential vorticity) in the vicinity of the upper level cyclone (see the Appendix).

An understanding the factors affecting the Eulerian-mean circulation is needed when interpreting the response to climate change. For example, it is known that the Hadley circulation responds to interhemispheric asymmetries (e.g., meridional gradients, Kang et al. 2008, 2009). Here I have shown that the circulation responds to subtropical zonal asymmetries. Further research is required to better understand the relative roles of zonal-mean and asymmetric forcing in the variability of the Eulerian-mean circulation and in its response to climate change. The interannual variability of planetary-scale wave momentum transport is known to impact the general circulation (Caballero 2007; Grise and Thompson 2012). In response to changes in greenhouse gas concentrations there is a robust land-ocean surface warming contrast (Manabe et al. 1991) in addition the NH subtropical anticyclones are expected to intensify (Li et al. 2012).

The importance of monsoon-anticyclone latent heat and momentum transport in setting the poleward boundary of the cross-equatorial circulation, including precipitation in the NH is consistent with previous studies. (Chou and Neelin 2003; Privé and Plumb 2007b). Privé and Plumb (2007b) noted that MSE transport limits the poleward extent of the monsoon by advecting low MSE air from the midlatitude oceans. Here the poleward boundary of the circulation was co-located with maximum planetary-scale streamfunction variance. The zonal-mean sub-cloud moist entropy moves southward in response to a subtropical forcing due to wave transport where as the boundary of the circulation moves northward. Note however that the global moist entropy maximum did provide some insight into the transition to a thermally-direct circulation suggesting that a three-dimensional representation of the monsoon is also relevant.

The aquaplanet model simulations provide insight into the dynamics of the NH seasonal transition and can be used to interpret the differences between the evolution in the NH and SH. The SH planetary-scale wave transport (and wave streamfunction variance) in the lower troposphere is weaker and of a higher zonal wavenumber than in the NH. Consistently the subtropical waviness is weaker, the seasonal transition is less abrupt, and the westward zonal wind in the upper troposphere and jet shift are weaker. While the aquaplanet model simulations provided significant insight, there are limitations. In particular, the simulations involved an imposed SST forcing and thus cannot be used to understand the processes that amplify the wave streamfunction and transport. In the real atmosphere the evolution of solar insolation and feedbacks with the land surface can amplify the temperature and thus the wave streamfunction and transport. The planetary-scale wave transport was underestimated in the aquaplanet simulations because the lack of a realistic land surface weakens the wave latent heat transport (there is no equatorward advection of relatively dry air), which likely affects the threshold condition for the circulation transition. Along similar lines, the simulations did not account for key features associated with the NH monsoons e.g., the asymmetry of the monsoons (dominance of the Asian monsoon system), land surface feedbacks (Cook 2003), ocean dynamics (Clement 2006) and the interaction with topography (e.g., Boos and Kuang 2010; Park et al. 2012). In addition the transition in the aquaplanet simulations depends on the parameterization of convection (parameterized versus large scale condensation). Future work will focus on the role of surface heat capacity, evaporation, topography, ocean heat transport, and convective parameterization in the seasonal transition.

Finally, current theories of the general circulation in the tropics assume angular momentum conservation (e.g., Held and Hou 1980) and thus do not account for the role of planetary-scale wave momentum and latent heat transport. The present results show that the monsoon-anticyclone system should be included in theories of the general circulation on Earth. A promising direction in that respect is to extend zonally-symmetric results to non-symmetric flows that obey QG dynamics following Emanuel (1995). The quasi-linear dependence of planetary-scale wave transport on wave streamfunction variance is promising for creating a diffusive model following Kushner and Held (1998) and Held (1999). Extending current theories to include the fundamental role of planetary-scale wave transport in the Eulerian-mean meridional circulation in order to better understand its response to climate change is work in progress.

APPENDIX

Seasonal transition of upper tropospheric absolute vorticity and potential vorticity

The abrupt circulation transition in the CAM5 aquaplanet model simulations discussed in Section 4 coincide with a reversal of absolute vorticity in the NH tropics (see Fig. 7, bottom, right). Here we show that this behavior is consistent with the NH seasonal transition in ERA-Interim reanalysis data.

The seasonal evolution of minimum absolute vorticity at 150 hPa and minimum potential vorticity at 370 K in the NH in the ERA-Interim data set are shown in Fig. 15 (top). Negative absolute and potential vorticity occur during winter consistent with advection by the NH winter Hadley circulation. During the seasonal transition, beginning around day 100, negative absolute vorticity (and potential vorticity) develops between 120 and 180°W, which is south of the upper level cyclone and in the vicinity of north-east flow (see Fig. 4, top, right). The co-location of the negative vorticity and upper level cyclone in the NH tropics is consistent with the CAM5 aquaplanet model simulations discussed in Section 4 (see green line in bottom panel of Fig. 11). Note that the appearance of negative absolute vorticity in ERA-Interim precedes the abrupt seasonal transition of the zonal-mean vertical motion at 900 hPa, which occurs around day 135 (see red line Fig. 2, right) and is also consistent with the aquaplanet model experiments. The absolute vorticity subsequently strengthens as the SH Hadley cell advects positive vorticity southward. Note that the negative absolute vorticity is maintained in the CAM5 simulations because of the constant SST forcing. The JJA averaged absolute vorticity at 150 hPa and potential vorticity at 370 K (Fig. 15, bottom) show that while the absolute vorticity and potential vorticity are low in the vicinity of the upper level Tibetan anticyclone, the minimum vorticity occurs between 120 and 180°W during NH summer. The consistency between the ERA-Interim and CAM5 aquaplanet model in terms of their absolute vorticity is reflected in the similarity of their precipitation and its coupling to the streamfunction in the lower troposphere (see Fig. 16). The precipitation response in CAM5 suggests a transition from an oceanic ITCZ to a land ITCZ.

Acknowledgments.

TAS thanks Drs. O. Pauluis, I. Simpson and M. Ting for helpful comments on the manuscript, Drs. O. Pauluis, R. A. Plumb, T. Schneider, R. Seager, A. H. Sobel and M. Ting for helpful discussions and Dr. W. R. Boos and B. Dobbins for help with the CAM5 simulations. TAS gratefully acknowledges financial support from the National Science Foundation (grant no. AGS-125520) and from the David and Lucile Packard Foundation. The author thanks the ECMWF for providing the ERA-Interim reanalysis dataset and is grateful to two anonymous reviewers whose insightful comments lead to significant improvements of the manuscript.

REFERENCES

Boos, W. R. and Z. Kuang, 2010: Dominant control of the south Asian monsoon by orographic insulation versus plateau heating. *Nature*, **464**, doi:10.1038/nature08707.

Bordoni, S. and T. Schneider, 2008: Monsoons as eddy-mediated regime transitions of the tropical overturning circulation. *Nature Geosc.*, **1**, 515–519.

Caballero, R., 2007: Role of eddies in the interannual variability of Hadley cell strength. *Geophys. Res. Lett.*, **34**, doi:10.1029/2007GL030971.

Caballero, R., 2008: Hadley cell bias in climate models linked to extratropical eddy stress. *Geophys. Res. Lett.*, **35**, doi:10.1029/2008GL035084.

Chao, W. C. and B. Chen, 2001: The origin of monsoons. *J. Climate*, **58**, 3497–3507.

Charney, J. G. and P. G. Drazin, 1961: Propagation of planetary-scale disturbances from the lower into the upper atmosphere. *J. Geophys. Res.*, **66**, 83–109.

Chen, T.-C., 2003: Maintenance of summer monsoon circulations: A planetary-scale perspective. *J. Climate*, **16**, 2022–2037.

Chen, T.-C., 2010: Characteristics of summer stationary waves in the northern hemisphere. *J. Climate*, **23**, 4489–4507.

Chou, C. and J. D. Neelin, 2003: Mechanisms limiting the northward extent of the northern summer monsoons over North America, Asia, and Africa. *J. Climate*, **16**, 406–425.

Clement, A. C., 2006: The role of the ocean in the seasonal cycle of the Hadley circulation. *J. Atmos. Sci.*, **63**, 3351–3365.

Collins, W., P. J. Rasch, B. A. Boville, J. J. Hack, J. R. McCaa, D. L. Williamson, and B. P. Briegleb, 2006: The formulation and atmospheric simulation of the Community Atmosphere Model: CAM3. *J. Climate*, **19**, 2144–2161.

Cook, K. H., 2003: The role of continents in driving the Hadley cell. *J. Atmos. Sci.*, **60**, 957–976.

Dee, D. P., et al., 2011: The ERA-Interim reanalysis: configuration and performance of the data assimilation system. *Quart. J. R. Meteor. Soc.*, **137**, 553–597.

Dima, I. M., J. M. Wallace, and I. Kraucunas, 2005: Tropical zonal momentum balance in the NCEP reanalyses. *J. Atmos. Sci.*, **62**, 2499–2513.

Emanuel, K. A., 1995: On thermally direct circulations in moist atmospheres. *J. Atmos. Sci.*, **52**, 1529–1534.

Frierson, D. M. W., I. M. Held, and P. Zurita-Gotor, 2006: A gray-radiation aquaplanet moist GCM. Part I: Static stability and eddy scale. *J. Atmos. Sci.*, **63**, 2548–2566.

Gadgil, S., 2003: The Indian monsoon and its variability. *Annu. Rev. Earth Planet. Sci.*, **31**, 429–467.

Gill, A. E., 1980: Some simple solutions for heat-induced tropical circulation. *Quart. J. R. Met. Soc.*, **106**, 447–462.

Grise, K. M. and D. W. J. Thompson, 2012: Equatorial planetary waves and their signature in atmospheric variability. *J. Atmos. Sci.*, **69**, 857–874.

Held, I. M., 1999: The macroturbulence of the troposphere. *Tellus*, **51**, 59–70.

Held, I. M. and A. Czaja, 2012: Deconstructing the Hadley cell transport. *Q. J. Roy. Met. Soc.*, doi:10.1002/qj.2085.

Held, I. M. and A. Y. Hou, 1980: Nonlinear axially symmetric circulations in a nearly inviscid atmosphere. *J. Atmos. Sci.*, **37**, 515–533.

Held, I. M. and P. J. Phillips, 1990: A barotropic model of the interaction between the Hadley cell and a Rossby wave. *J. Atmos. Sci.*, **47**, 856–869.

Held, I. M., M. Ting, and H. Wang, 2002: Northern winter stationary waves: Theory and modeling. *J. Climate*, **15**, 2125–2144.

Juckes, M. N., 2000: The static stability of the midlatitude troposphere: The relevance of moisture. *J. Atmos. Sci.*, **57**, 3050–3057.

Kang, S. M., D. M. W. Frierson, and I. M. Held, 2009: The tropical response to extratropical thermal forcing in an idealized GCM: The importance of radiative feedbacks and convective parameterization. *J. Atmos. Sci.*, **66**, 2812–2827.

Kang, S. M., I. M. Held, D. M. W. Frierson, and M. Zhao, 2008: The response of the ITCZ to extratropical thermal forcing: Idealized slab-ocean experiments with a GCM. *J. Climate*, **21**, 3521–3532.

Kelly, P. and B. Mapes, 2011: Zonal mean wind, the Indian monsoon, and July drying in the western Atlantic subtropics. *J. Geophys. Res.*, **116**, doi:10.1029/2010JD015405.

Kelly, P. and B. Mapes, 2013: Asian monsoon forcing of subtropical easterlies in the Community Atmosphere Model: Summer climate implications for the western Atlantic. *J. Climate*, **26**, 2741–2755.

Kraucunas, I. and D. L. Hartmann, 2005: Equatorial superrotation and the factors controlling the zonal-mean zonal winds in the tropical upper troposphere. *J. Atmos. Sci.*, **62**, 371–389.

Kraucunas, I. and D. L. Hartmann, 2007: Tropical stationary waves in a nonlinear shallow-water model with realistic basic states. *J. Atmos. Sci.*, **64**, 2540–2557.

Kushner, P. J. and I. Held, 1998: A test, using atmospheric data, of a method for estimating oceanic eddy diffusivity. *Geophys. Res. Lett.*, **25**, 4213–4216.

Lee, S., 1999: Why are the climatological zonal winds easterly in the equatorial upper troposphere? *J. Atmos. Sci.*, **56**, 1353–1363.

Li, W., L. Li, M. Ting, and Y. Liu, 2012: Intensification of northern hemisphere subtropical highs in a warming climate. *Nature Geosc.*, **5**, 830–834.

Lindzen, R. S. and A. Y. Hou, 1988: Hadley circulations for zonally averaged heating centered off of the equator. *J. Atmos. Sci.*, **45**, 2416–2427.

Manabe, S., R. J. Stouffer, M. J. Spelman, and K. Bryan, 1991: Transient responses of a coupled ocean-atmosphere model to gradual changes of atmospheric CO2. Part I: Annual mean response. *J. Climate*, **4**, 785–818.

Neale, R. and B. J. Hoskins, 2001: A standard test for AGCMs including their physical parametrizations: I: The proposal. *Atmos. Sci. Lett.*, **1**, doi:10.1006/asle.2000.0019.

Neale, R., et al., 2010: Description of the NCAR Community Atmosphere Model (CAM 5.0). Tech. rep., Natl. Cent. for Atmos. Res., Boulder, Colo., 282 pp.

Park, H.-S., J. C. H. Chiang, and S. Bordoni, 2012: The mechanical impact of the Tibetan plateau on the seasonal evolution of the south Asian monsoon. *J. Climate*, **25**, 2394–2407.

Pauluis, O., T. A. Shaw, and F. Laliberte, 2011: A statistical generalization of the transformed Eulerian-mean circulation for an arbitrary vertical coordinate system. *J. Atmos. Sci.*, **68**, 1766–1783.

Peixoto, J. P. and A. H. Oort, 1992: *Physics of climate*. American Institute of Physics, 520 pp.

Plumb, R. A., 2007: Dynamical constraints on monsoon circulations. *The Global Circulation of the Atmosphere*, T. Schneider and A. Sobel, Eds., Princeton University Press, 252–266.

Plumb, R. A. and A. Y. Hou, 1992: The response of a zonally symmetric atmosphere to subtropical thermal forcing: Threshold behavior. *J. Atmos. Sci.*, **49**, 1790–1799.

Privé, N. and R. A. Plumb, 2007a: Monsoon dynamics with interactive forcing. Part I: Axisymmetric studies. *J. Atmos. Sci.*, **64**, 1417–1430.

Privé, N. and R. A. Plumb, 2007b: Monsoon dynamics with interactive forcing. Part II: Impact of eddies and asymmetric geometries. *J. Atmos. Sci.*, **64**, 1431–1442.

Randel, W. J. and I. M. Held, 1991: Phase speed spectra of transient eddy fluxes and critical layer absorption. *J. Atmos. Sci.*, **48**, 688–697.

Rodwell, M. J. and B. J. Hoskins, 1996: Monsoons and the dynamics of deserts. *Q. J. Roy. Met. Soc.*, **122**, 1385–1404.

Rodwell, M. J. and B. J. Hoskins, 2001: Subtropical anticyclones and summer monsoons. *J. Climate*, **15**, 3192–3211.

Schneider, E. K., 1987: A simplified model of the modified Hadley circulation. *J. Atmos. Sci.*, **44**, 3311–3328.

Schneider, E. K. and I. G. Watterson, 1984: Stationary Rossby wave propagation through easterly layers. *J. Atmos. Sci.*, **41**, 2069–2083.

Schneider, T., 2006: The general circulation of the atmosphere. *Annu. Rev. Earth Planet. Sci.*, **34**, 655–688.

Schneider, T. and S. Bordoni, 2008: Eddy-mediated regime transitions in the seasonal cycle of a Hadley circulation and implications for monsoon dynamics. *J. Atmos. Sci.*, **65**, 915–934.

Shaw, T. A. and O. Pauluis, 2012: Tropical and subtropical meridional latent heat transports by disturbances to the zonal mean and their role in the general circulation. *J. Atmos. Sci.*, **69**, 1872–1889.

Trenberth, K. E., D. P. Stepaniak, and J. M. Caron, 2000: The global monsoon as seen through the divergent atmospheric circulation. *J. Climate*, **13**, 3969–3993.

Webster, P. and J. Fasullo, 2003: Monsoon: Dynamical theory. *Encyclopedia of Atmospheric Sciences*, **3**, 1370–1391.

Wu, Y. and O. Pauluis, 2013a: Examination of isentropic circulation response to a doubling of carbon dioxide using Statistical Transformed Eulerian Mean. *J. Atmos. Sci.*, **70**, 1649–1667.

Wu, Y. and O. Pauluis, 2013b: Midlatitude tropopause and low-level moisture. Part I: Results from reanalysis datasets. *J. Atmos. Sci.*, submitted.

Zheng, X., 1998: The response of a moist zonally symmetric atmosphere to subtropical surface temperature perturbation. *Quart. J. Roy. Meteor. Soc.*, **124**, 1209–1226.

List of Figures

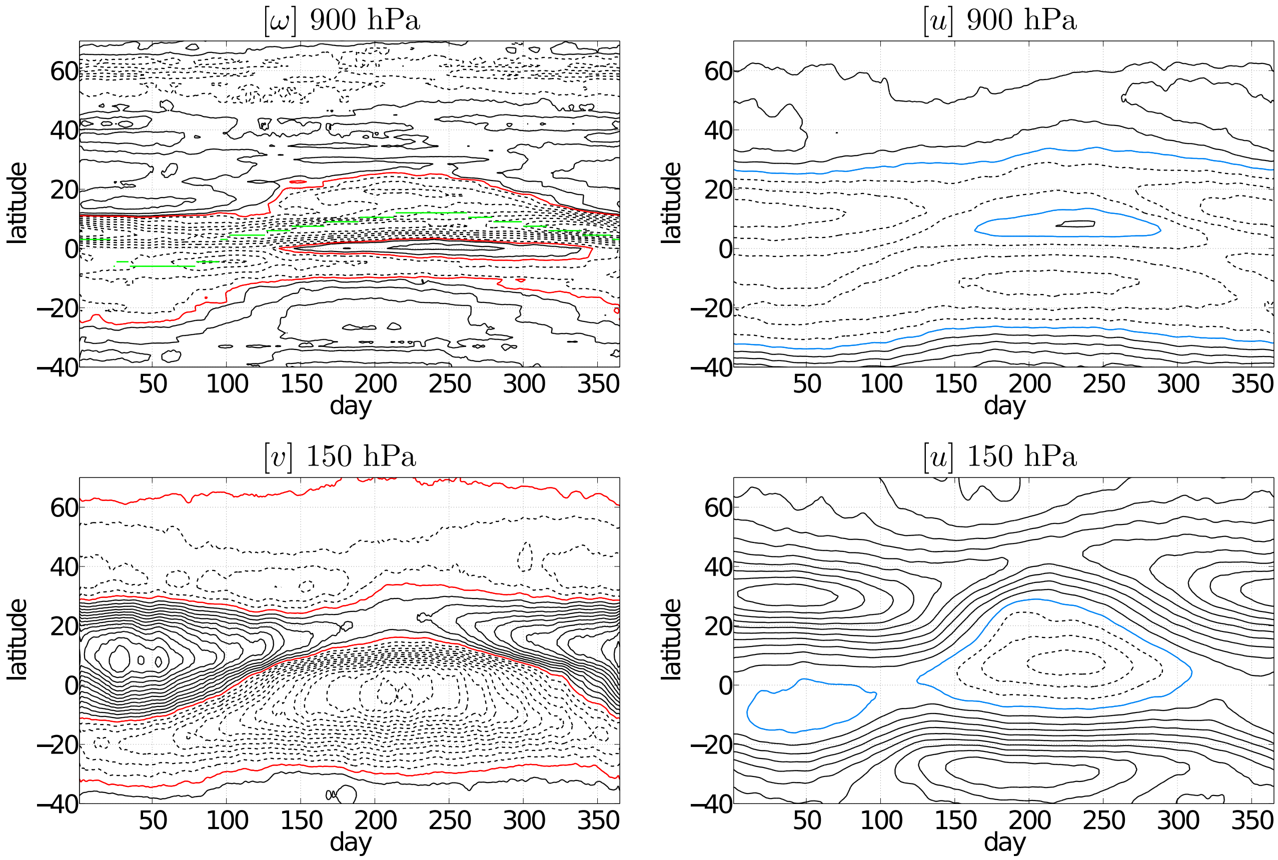

Fig. 1. Seasonal cycle of the zonal-mean flow in ERA-Interim. Top: Zonal-mean vertical (left) and zonal (right) wind at 900 hPa. Contour interval is 3.e-3 Pas^{-1} (left) and 2 ms^{-1} (right). Bottom: Zonal-mean meridional (left) and zonal (right) wind at 150 hPa. Contour interval is 0.2 ms^{-1} (left) and 4 ms^{-1} (right). The red lines indicates the zero contour for the zonal-mean vertical wind at 900 hPa (top) and meridional wind at 150 hPa (bottom). The green line indicates the location of the maximum equivalent potential temperature in the tropics at 900 hPa. The blue lines indicates the zero contour for the zonal-mean zonal wind at 900 hPa (top) and 150 hPa (bottom).

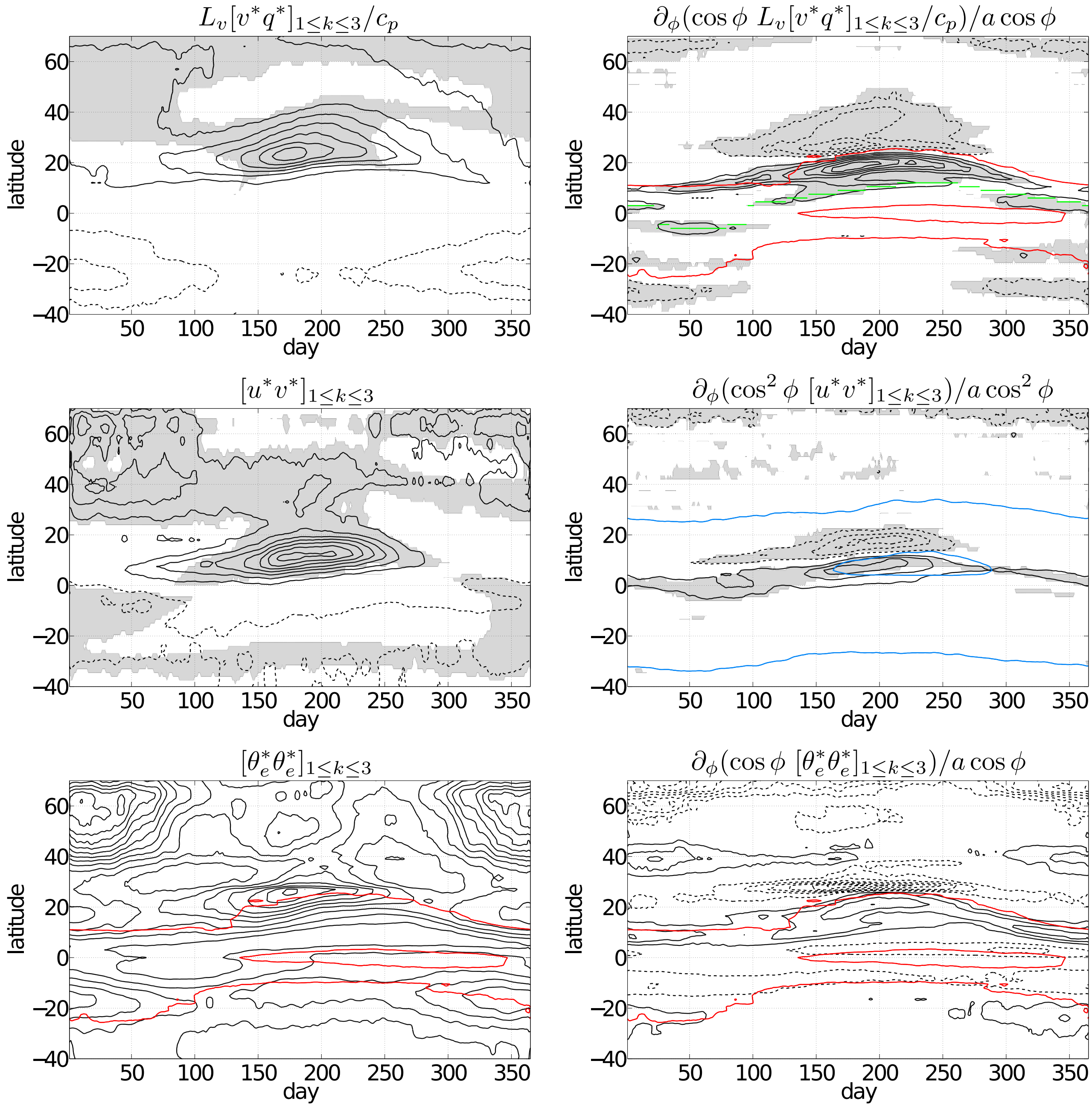

FIG. 2. Seasonal cycle at 900 hPa in ERA-Interim. Top: Planetary-scale wave latent heat transport (left) and meridional flux divergence (right). Contour intervals are 4.0 Kms^{-1} and 0.4 Kday^{-1}, respectively. Middle: Planetary-scale wave momentum transport (left) and meridional flux divergence (right). Contour intervals are 2.0 m^{2}s^{-2} and 0.4 ms^{-1}day^{-1}, respectively. Bottom: Planetary-scale wave equivalent potential temperature variance (left) and meridional flux divergence (right). Contour intervals are 10.0 K^2 and 1.5 K^{2}m^{-1}, respectively. Negative contours are dashed. The colored lines are as in Fig. 1.

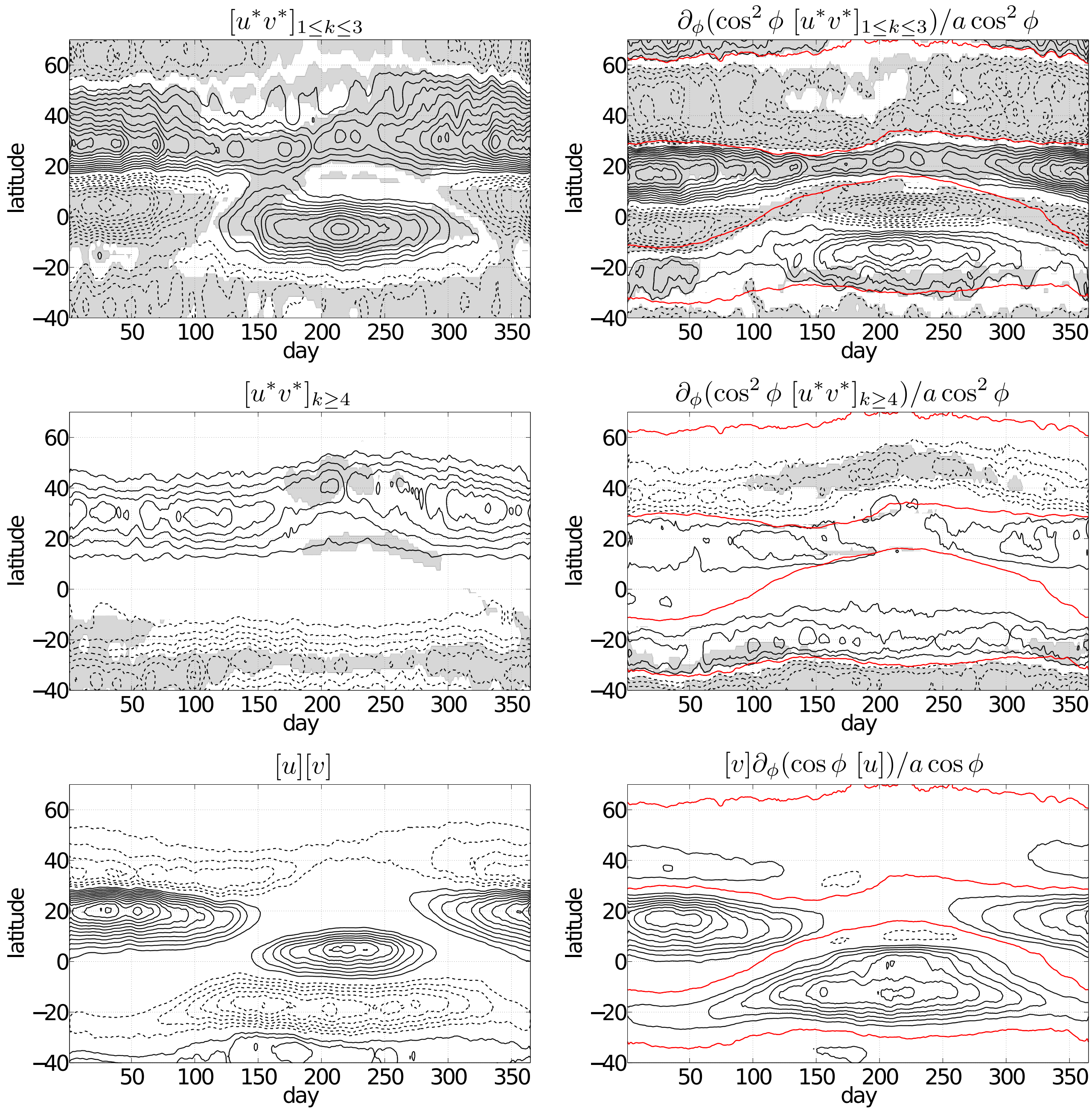

FIG. 3. Seasonal cycle at 150 hPa in ERA-Interim. Momentum transport (left) and flux divergence (right) by planetary (top) and subplanetary-scale (middle) waves and the zonal-mean flow (bottom). Shading indicates where planetary scale transport and its flux divergence dominate over the zonal-mean (top) and where subplanetary-scale transport and its flux divergence dominate over the sum of the zonal-mean and planetary-scale transport (middle). Contour intervals are 4.0 m^{2}s^{-2} (left) and 0.4 ms^{-1}day^{-1} (right) and negative contours are dashed. The red line corresponds to the zero line for the 150 hPa zonal-mean meridional wind.

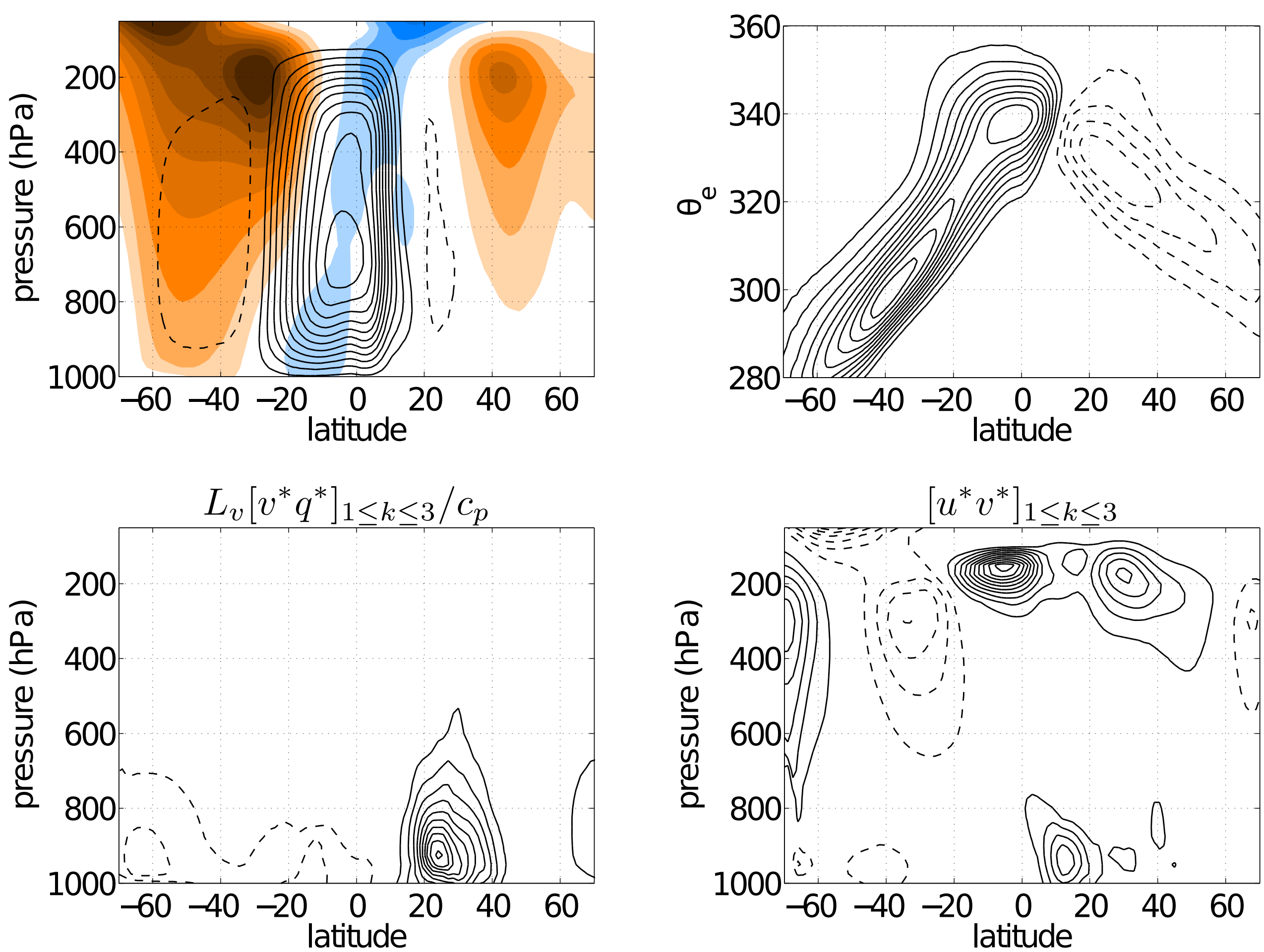

FIG. 4. Zonal-mean circulation during JJA in ERA-Interim. Top: Eulerian-mean circulation (black, left) and zonal-mean zonal wind (color, left) and moist isentropic circulation (right). Contour intervals are 2.e10 kgs^{-1} and 10.0 ms^{-1}, respectively and dashed contours indicate a clockwise circulation. Bottom: Planetary-scale wave latent heat (left) and momentum (right) transport. Contour intervals are 2.0 Kms^{-1} (left) and 2.0 m^{2}s^{-2} (right), respectively.

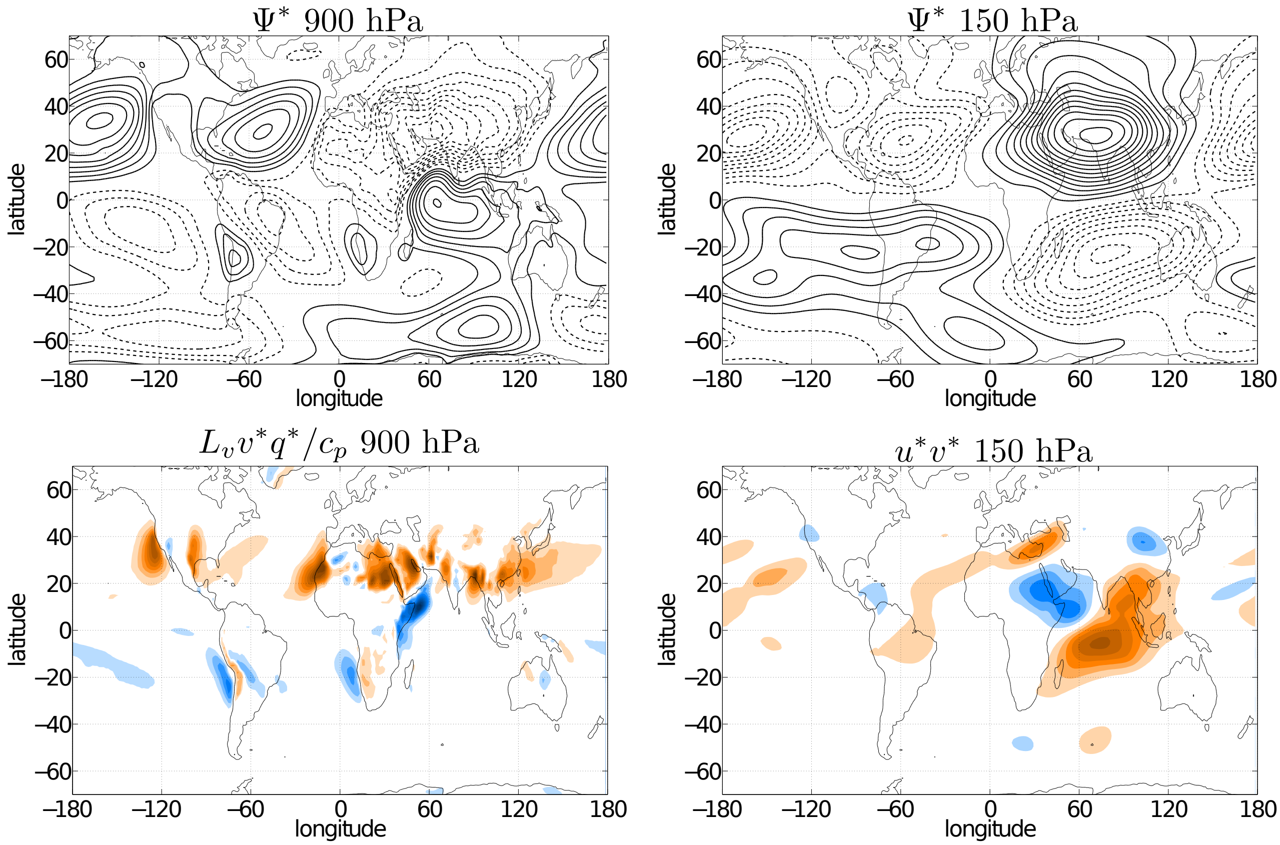

Fig. 5. Zonally-asymmetric circulation during JJA in ERA-Interim. Top: Zonally-asymmetric streamfunction at 900 hPa (left) and 150 hPa (right). Contour interval is 1.5e6 m^2s^{-1} (left) and 3.e6 m^2s^{-1} (right). Bottom: Zonal structure of the stationary wave latent heat transport at 900 hPa (left) and momentum transport at 150 hPa (right). Contour interval is 10 Kms^{-1} (left) and 10 m^2s^{-2} (right).

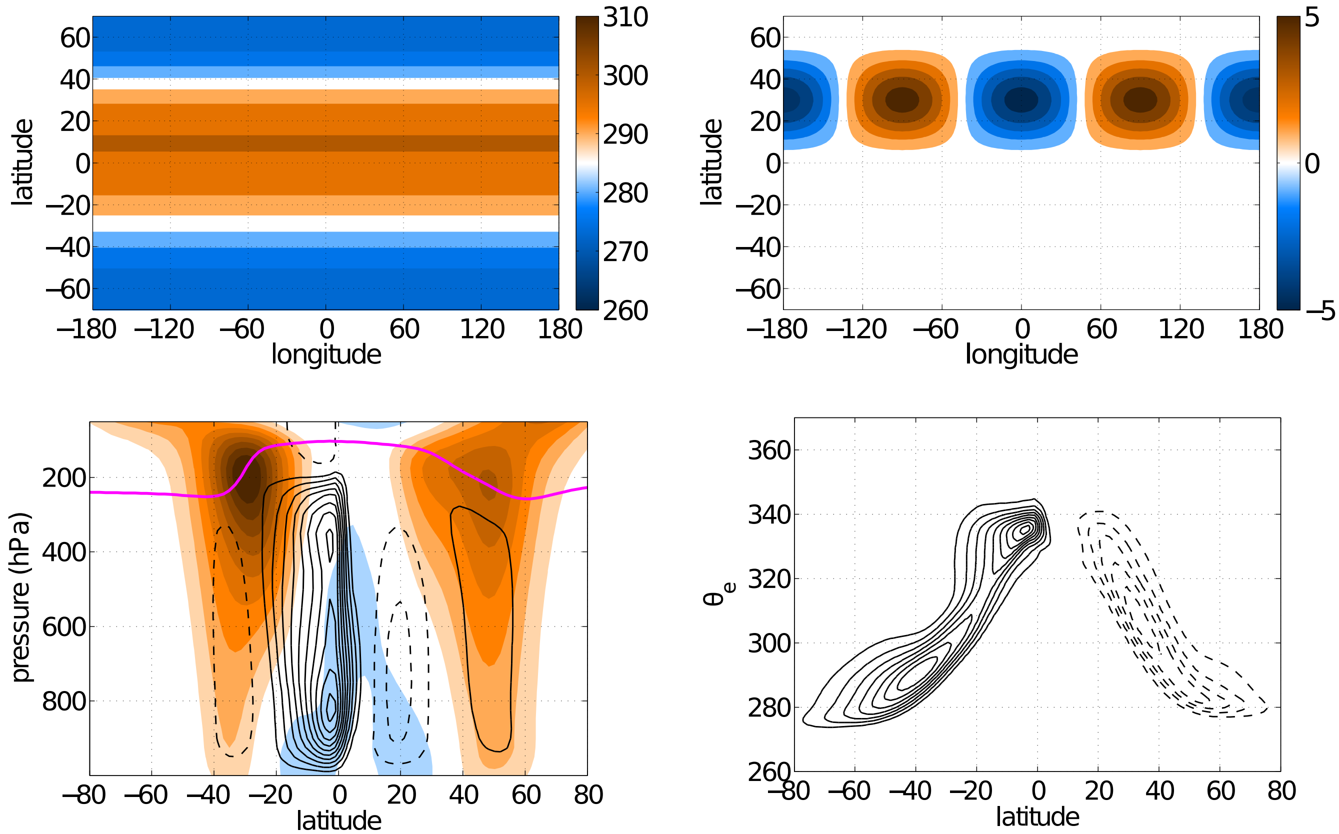

FIG. 6. Aquaplanet model configuration. Top: Zonal-mean 'Qobs' SST distribution with maximum SST shifted to 10°N (left) and wave-2 SST perturbation at 30°N (right). Bottom: Eulerian-mean circulation (left, black), zonal-mean zonal wind (left, color), tropopause (left, magenta) and moist-isentropic circulation (right) for the zonally-symmetric 'Qobs' SST. Circulation and zonal-mean zonal wind contour intervals are 3.e10 kgs^{-1} and 10 ms^{-1}, respectively.

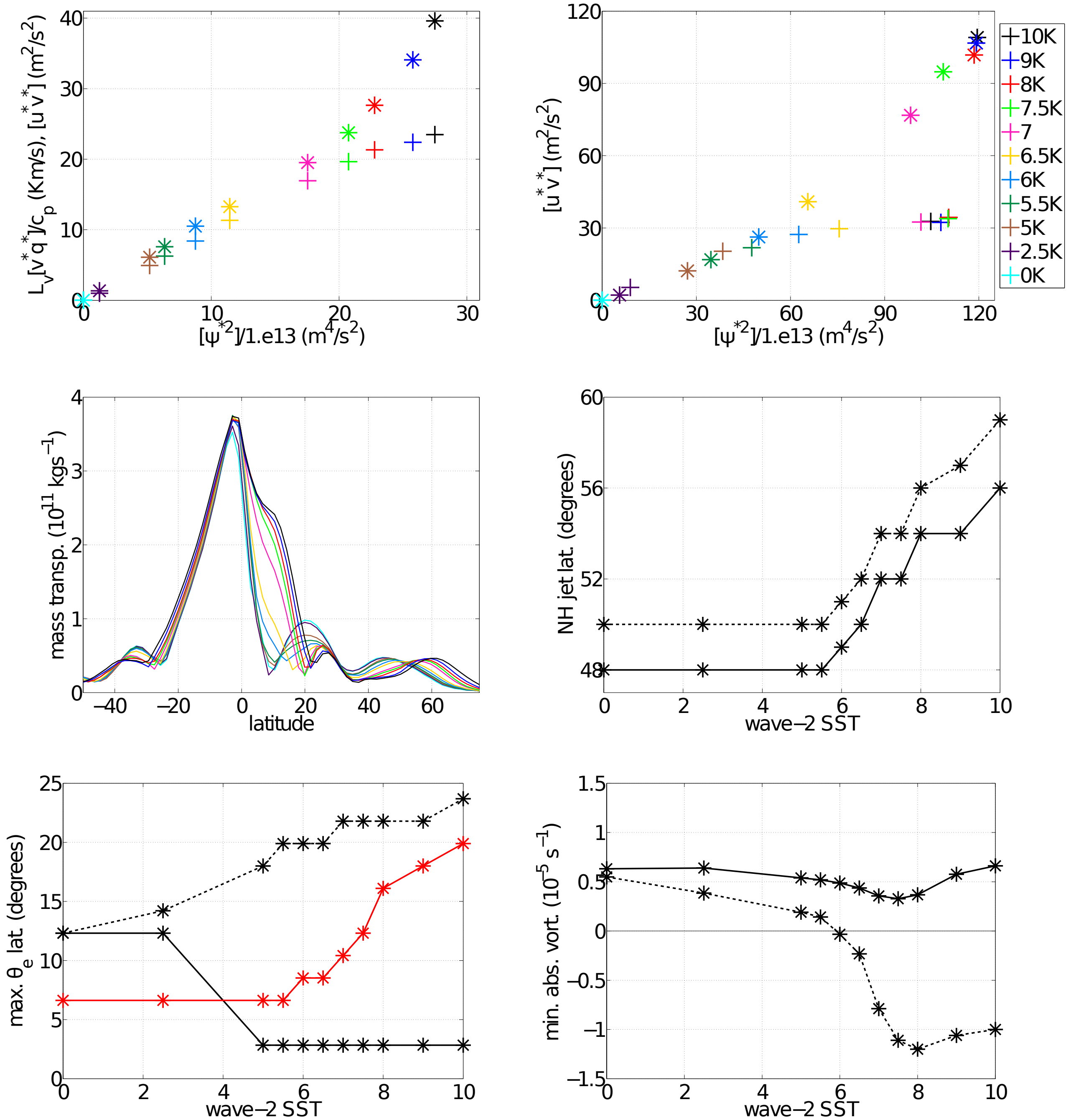

FIG. 7. Response of aquaplanet climate to wave-2 SST forcing. Top: Wave-2 latent heat (star) and momentum (plus) transport as a function of wave-2 streamfunction variance at 1000 hPa in the NH subtropics (left). Wave-2 momentum transport in the NH subtropics (plus) and tropics (star) as a function of wave-2 streamfunction variance at 150 hPa. Middle: Eulerian-mean mass transport (left) and latitude of the NH subtropical (solid) and eddy-driven (dashed) jet maxima (right). Bottom: Variation of maximum zonal-mean (solid) and global (dashed) equivalent potential temperature at 1000 hPa (left) and minimum zonal-mean (solid) and global (dashed) absolute vorticity in the NH (1 to 90°N) at 150 hPa. The location of zero Eulerian-mean streamfunction at 850 hPa is shown in red (left).

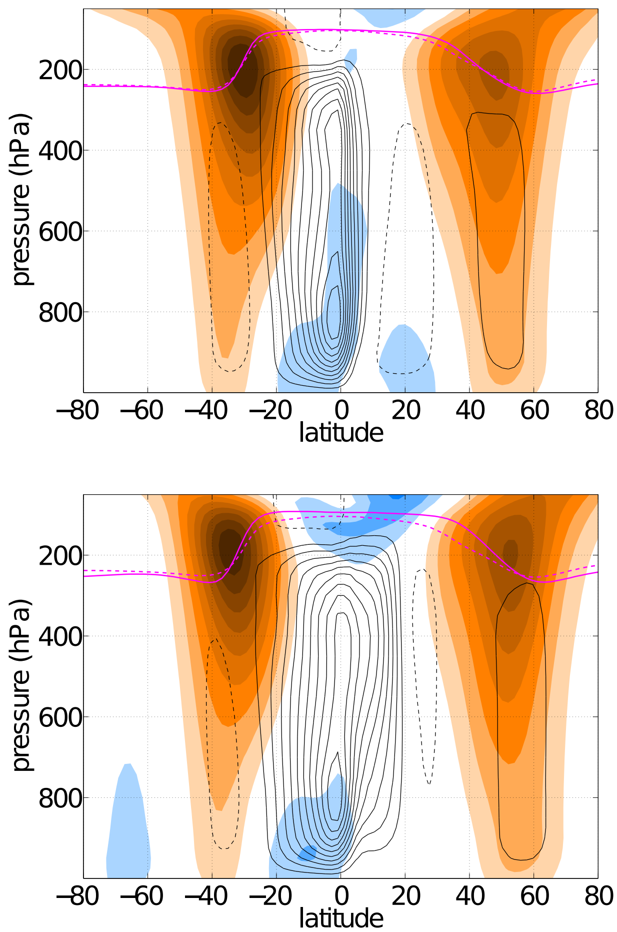

Fig. 8. Aquaplanet Eulerian-mean circulation (black), zonal-mean zonal wind (color), tropopause height (magenta) in response to a 5.5 (top, left) and 7.5 (bottom, left) K wave-2 SST forcing and difference from zonally-symmetric climate (right). The tropopause for the zonally-symmetric climate is indicated by the dashed magenta line and the corresponding circulation in Fig. 6 (bottom, left). Circulation and zonal-mean zonal wind contour intervals are 3.e10 kgs^{-1} and 10 ms^{-1} (left) and 1.e10*[1, 2, 4, 8, 16, 32] kgs^{-1} and 2.5 ms^{-1} (right).

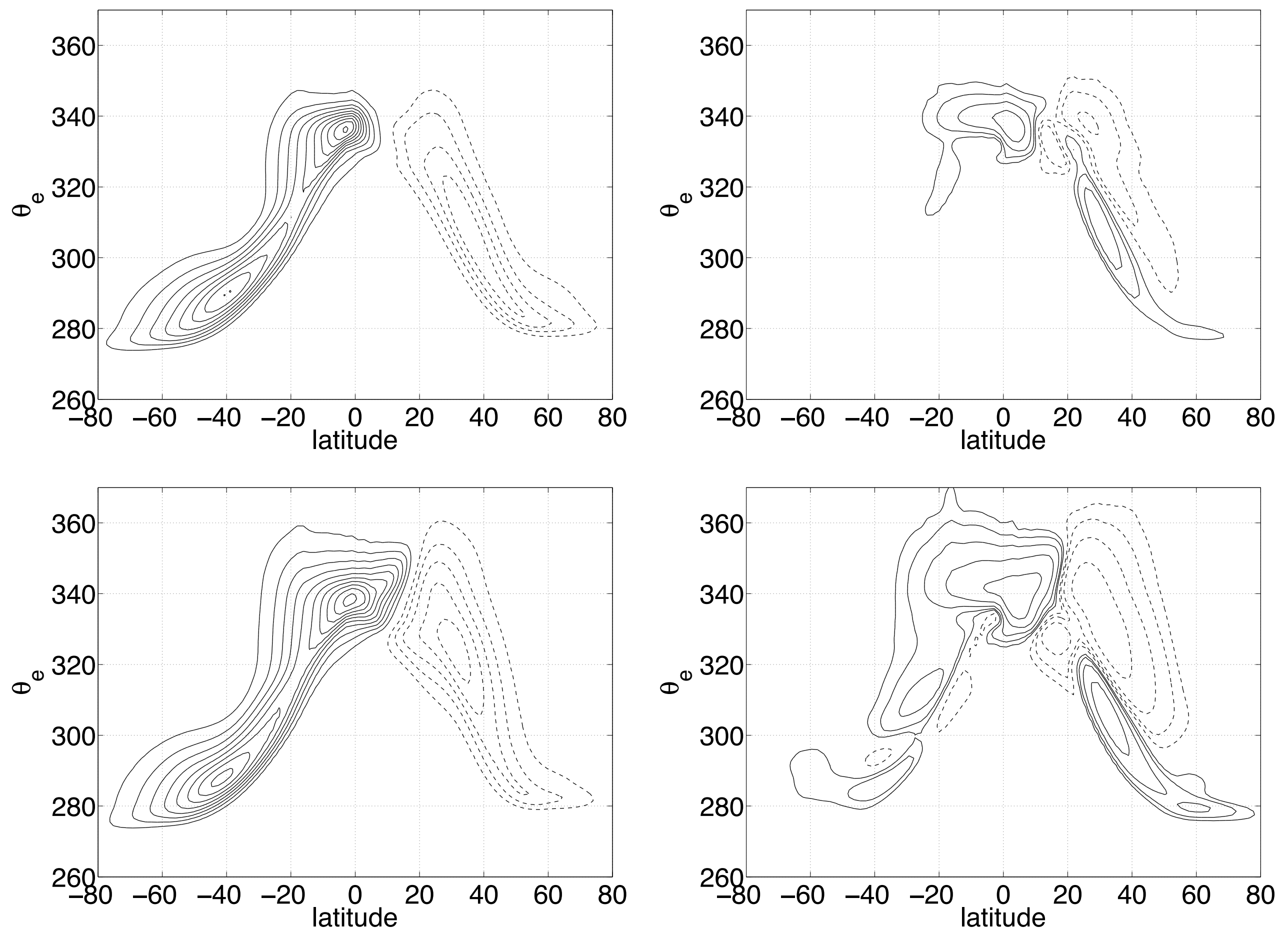

Fig. 9. Aquaplanet moist isentropic circulation response to a 5.5 (top, left) and 7.5 (bottom, left) K wave-2 SST forcing and difference from zonally-symmetric background state (right). Contour interval is 3.e10 kgs^{-1} (left) and 1.e10*[1, 2, 4, 8, 16, 32] kgs^{-1} (right).

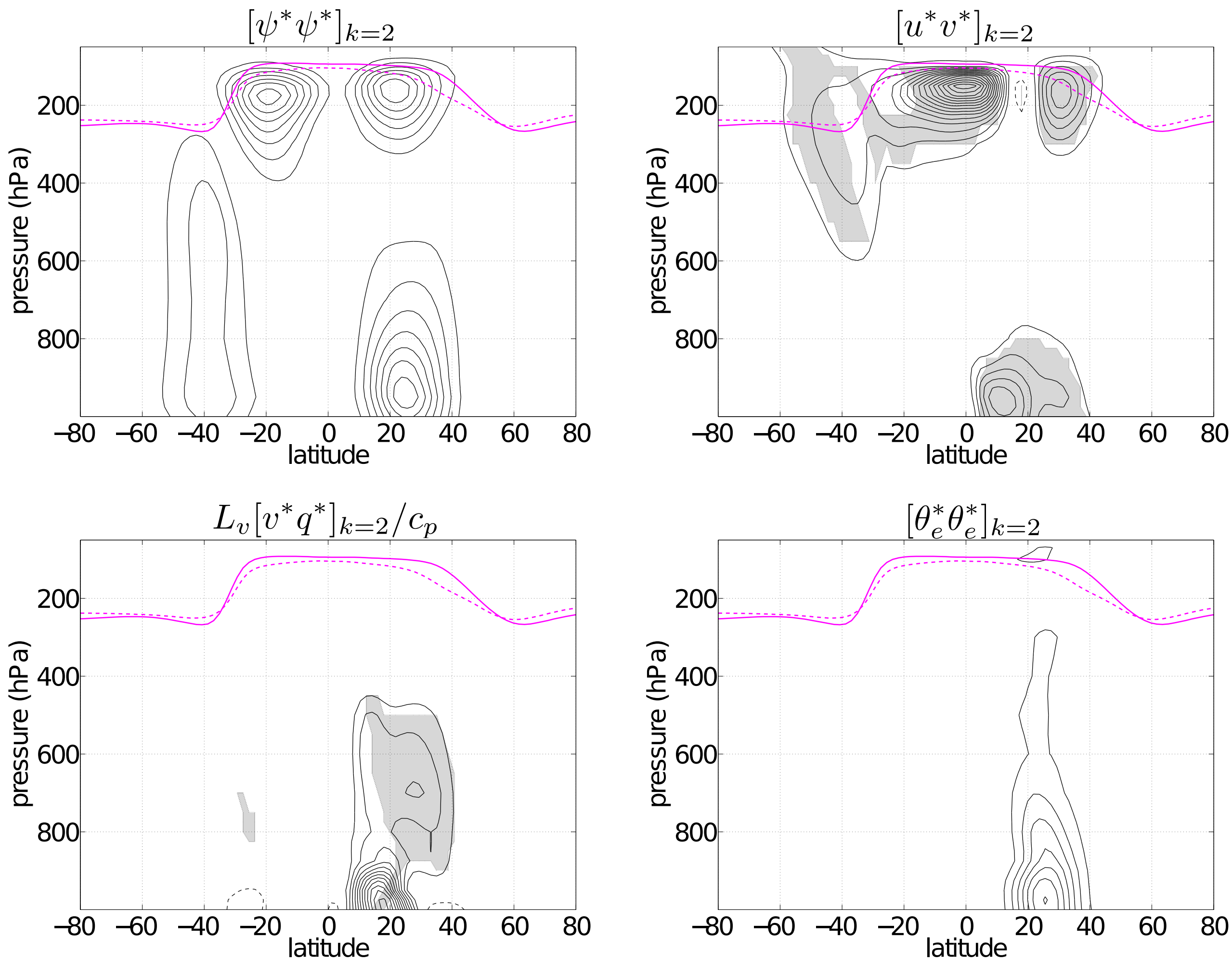

FIG. 10. Aquaplanet wave-2 response to 7.5 K wave-2 SST forcing. Top: Density-weighted streamfunction variance (left), momentum transport (right) response. Bottom: latent heat transport (left) and equivalent potential temperature variance (right) response. Shading indicates where wave-2 transport dominates over zonal-mean transport. Contour intervals are 2.e13 m^4s^{-2}, 6 m^2s^{-2}, 2 Kms^{-1}, and 30 $K^2m^2s^{-2}$.

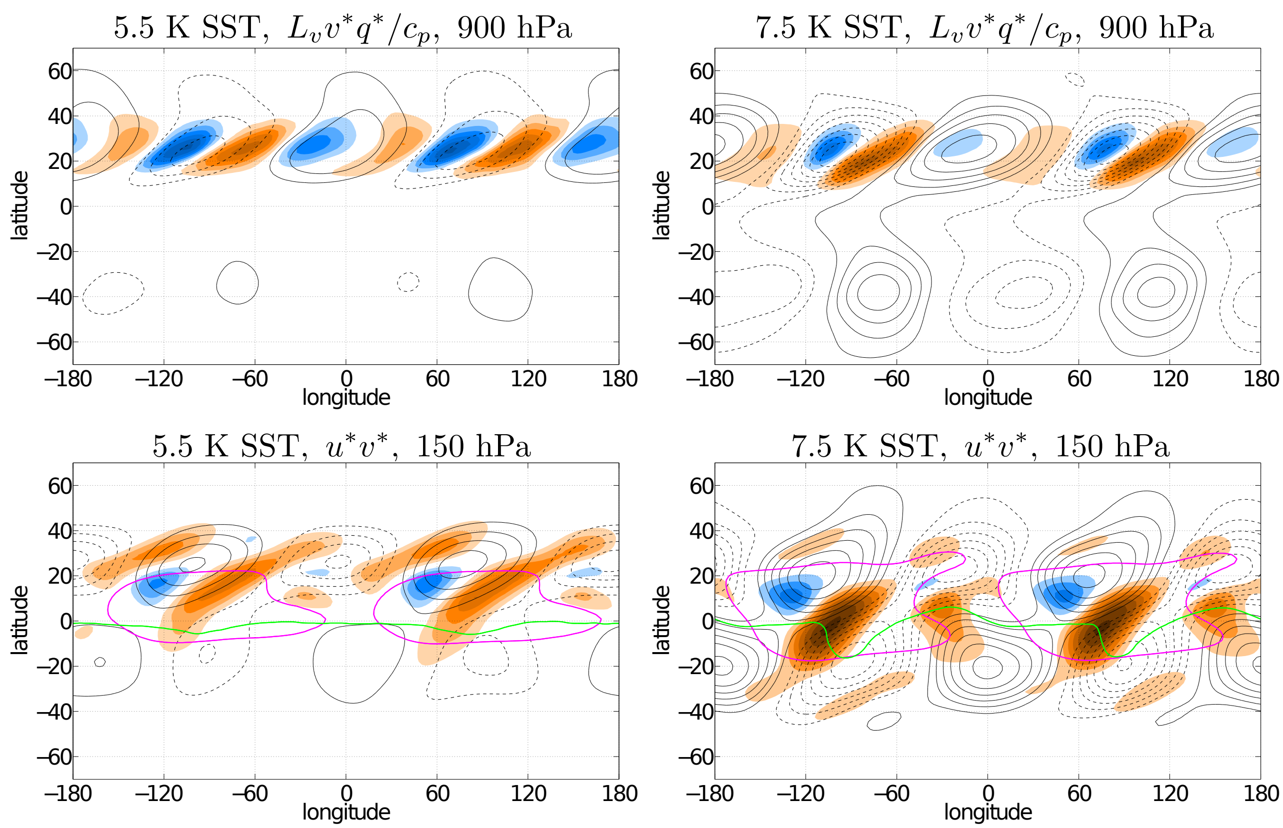

FIG. 11. Zonal structure of aquaplanet stationary wave transport response to 5.5 K (left) and 7.5 (right) K wave-2 SST forcing. Top: Latent heat transport (color) and streamfunction (black) at 900 hPa. Contour intervals are 2 $\mathrm{Kms^{-1}}$ (left) and 10 $\mathrm{Kms^{-1}}$ (right). Bottom: Momentum transport (color) and streamfunction (black) at 150 hPa. Contour intervals are 15 $\mathrm{m^2s^{-2}}$ (left) and 50 $\mathrm{m^2s^{-2}}$ (right). Streamfunction contour interval is 2.5e6 $\mathrm{m^2s^{-1}}$ (top) and 5.e6 $\mathrm{m^2s^{-1}}$ (bottom). The magenta and green lines indicates the zero contour for the zonal-mean zonal wind and absolute vorticity, respectively, at 150 hPa.

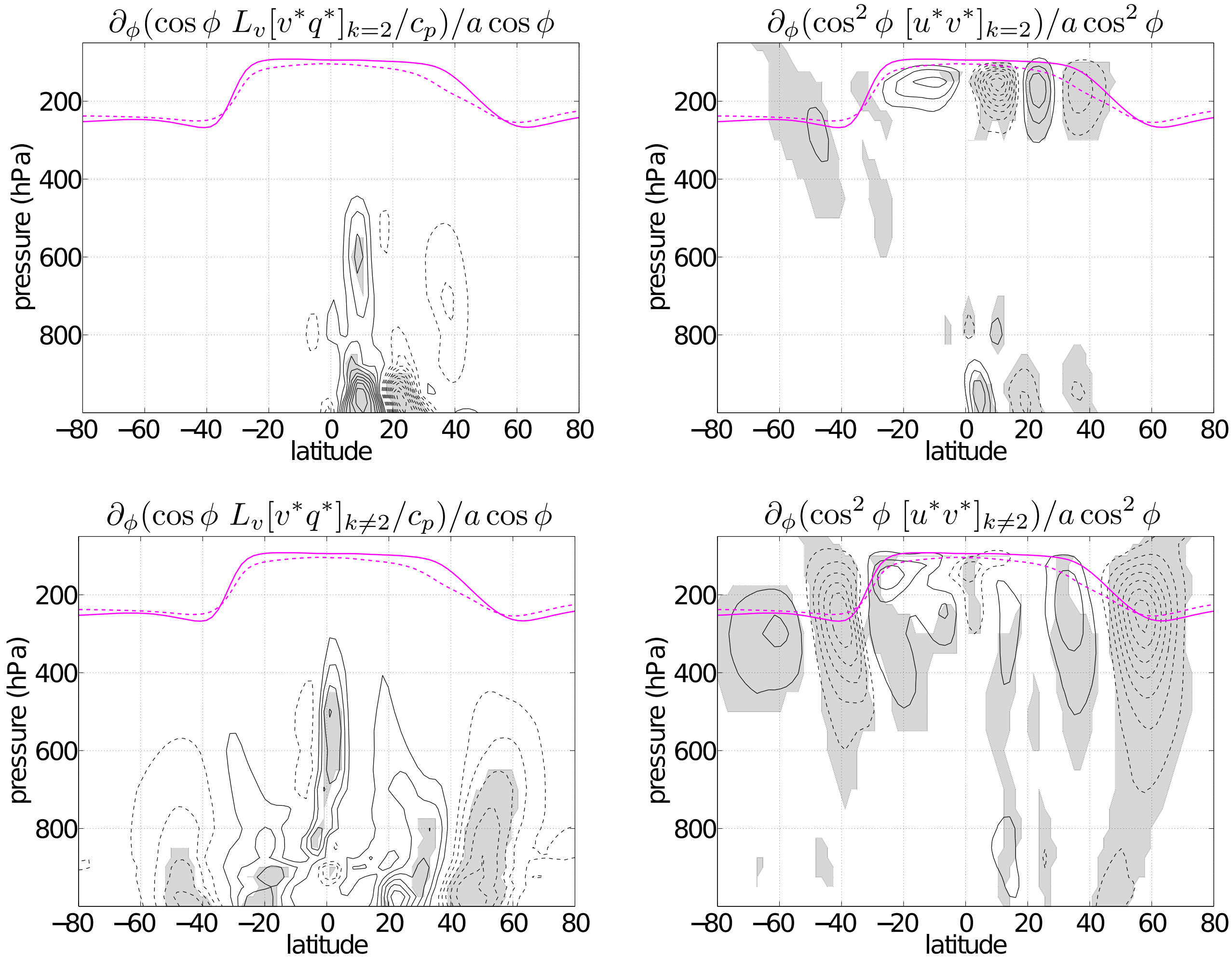

FIG. 12. Aquaplanet eddy flux divergence response to a 7.5 K wave-2 SST forcing. Top: Wave-2 latent heat (left) and momentum (right) meridional flux divergence. Shading indicates where wave-2 flux divergence dominates over the flux divergence by the zonal-mean flow. Bottom: Subplanetary-scale wave latent heat (left) and momentum (right) flux divergence. Shading indicates where subplanetary-scale transport and flux divergence dominate over the sum of the zonal-mean and planetary-scale divergence. Contour interval is 0.2 Kmday^{-1} (right) and 1 ms^{-1}day^{-1} (left) negative contours are dashed.

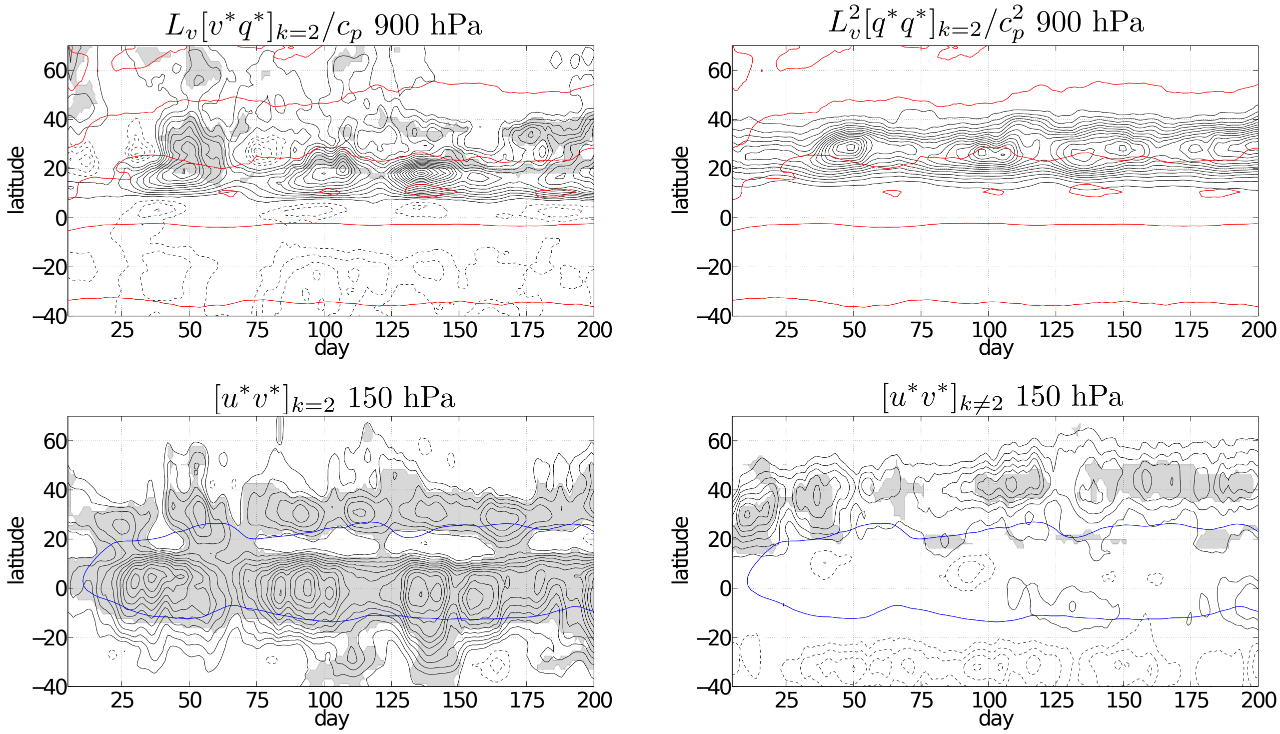

FIG. 13. Transient evolution of aquaplanet model response to a 7.5 K wave-2 SST forcing. Top: Wave-2 latent heat transport (left) and variance (right) at 900 hPa. Contour interval is 2.0 Kms^{-1} (left) and 10 K^2 (right). Bottom: Wave-2 (left) and subplanetary-scale (right) momentum transport at 150 hPa. Contour interval is 10 m^{2}s^{-2}. The red and blue lines correspond to the zero zonal-mean vertical wind at 900 hPa and zonal-mean zonal wind at 150 hPa, respectively.

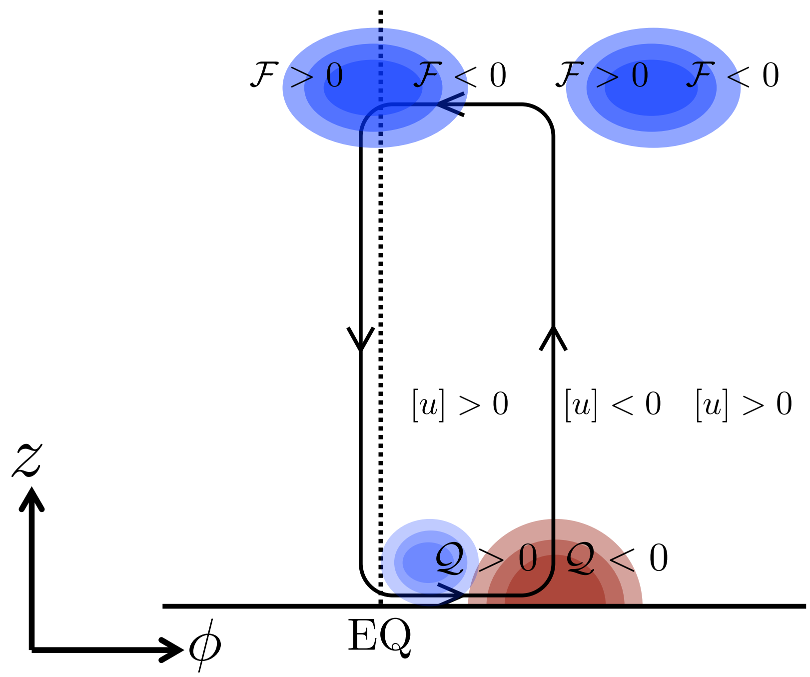

FIG. 14. Schematic of zonal-mean circulation response to a zonally-asymmetric surface forcing in the NH subtropics. Red (blue) regions indicate northward planetary-scale wave latent heat (momentum) transport. $\mathcal{F}$ and $\mathcal{Q}$ indicate the meridional flux divergence of meridional momentum and latent heat flux (torque and diabatic heating) induced by planetary-scale meridional wave momentum and latent heat flux divergences, respectively. $[u]$ represents the barotropic zonal-mean zonal wind response assuming a balance between $\mathcal{F}$ and surface friction.

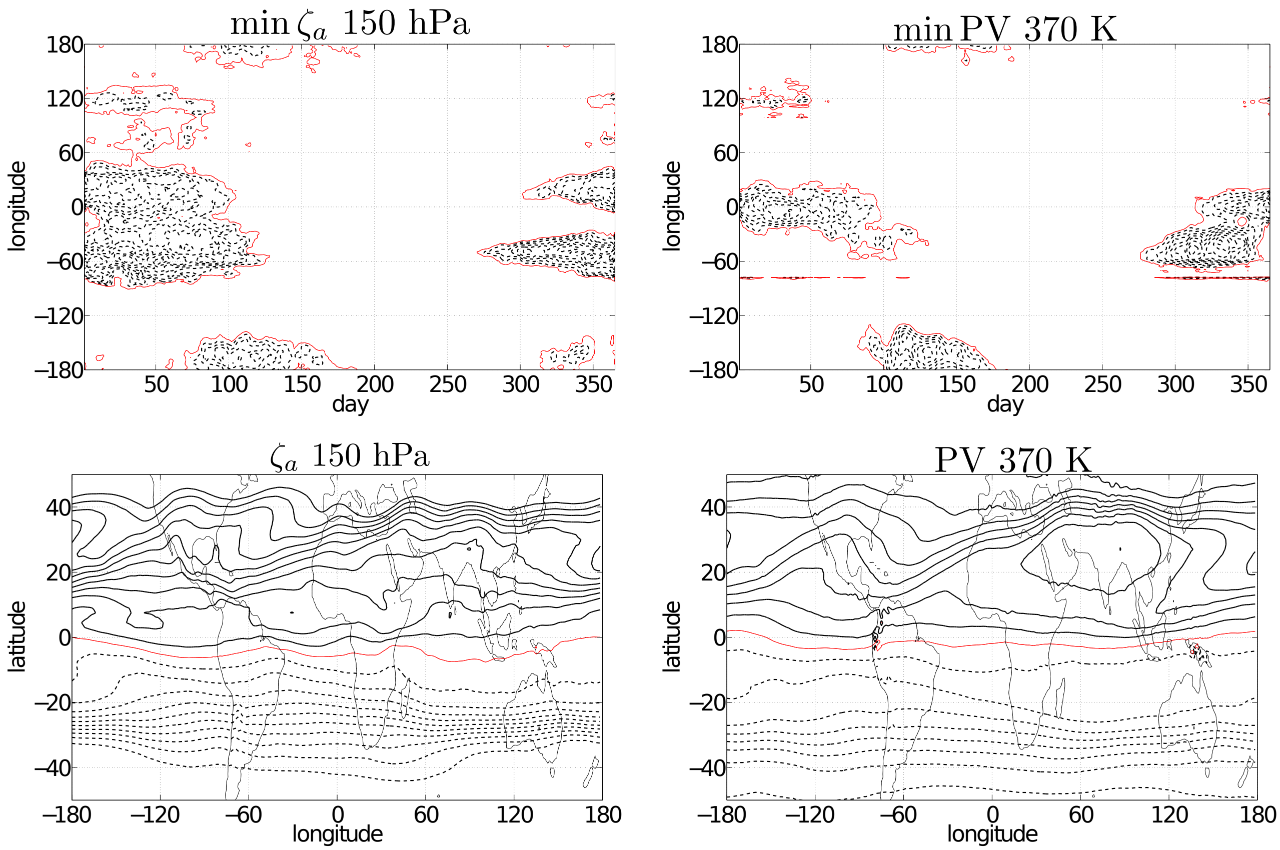

FIG. 15. Absolute vorticity at 150 hPa and potential vorticity at 370 K in ERA-Interim. Top: Seasonal cycle of the NH minimum value of absolute vorticity (left) and potential vorticity (right). Contour interval is 1.e-5 s^{-1} (left) and 1.e-7 $Km^2kg^{-1}s^{-1}$ (right). Bottom: Absolute vorticity (left) and potential vorticity during JJA. Contour interval is 1.e-5 s^{-1} (left) and 1.e-6 $Km^2kg^{-1}s^{-1}$ (right). The red line indicates the zero contour for the absolute or potential vorticity.

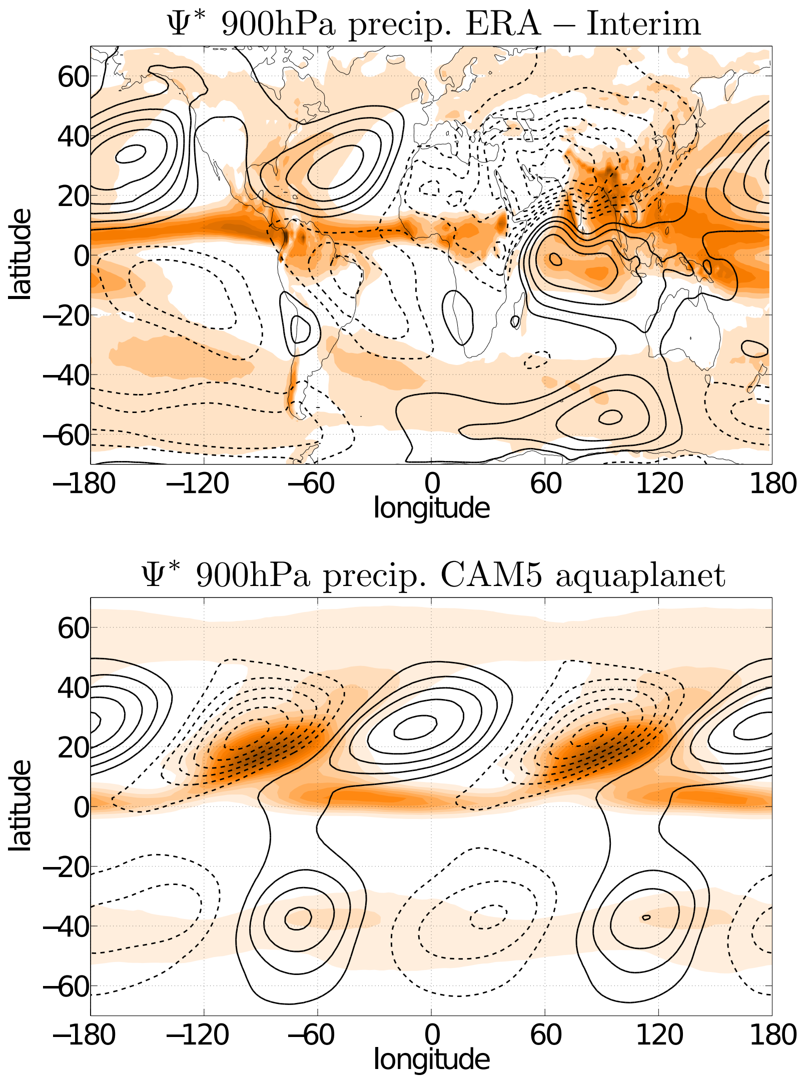

FIG. 16. ERA-Interim precipitation during JJA (top) and CAM5 aquaplanet model precipitation for the 7.5 K wave-2 SST forcing (bottom). Contour interval is 2 mmday^{-1}.